

# 7

## Active volcanism: Effusive eruptions

*David A. Williams and Robert R. Howell*

### 7.1 INTRODUCTION

Io's most remarkable characteristic is its active volcanism. Volcanic eruptions on Io consist of effusions of lava as long lava flows, as lava lakes, and as fire fountains, as well as explosive plumes of gas and dust. In this chapter we review the major types of eruptions thought to occur on Io, with emphasis on their extrusive components, based on the major results from the *Galileo* mission. These include the possible discovery of very high temperature lavas which are consistent with pre-historic terrestrial ultramafic lavas, evidence for silicate lava lakes and compound flow fields, and sulfur and possibly sulfur dioxide flows. In this context we also discuss the nature of several important volcanic centers as shown from *Galileo* high-resolution observations.

### 7.2 CONTEXT: TERRESTRIAL EFFUSIVE VOLCANISM

Effusive volcanism, exemplified by lava flows and lava lakes, is ubiquitous on Earth, and evidence of effusive volcanism is found throughout the geologic record, dating as far back as the Archean (e.g., De Witt and Ashwal, 1997). As on other planets, the products and emplacement styles of lava flows on Earth are dependent upon the volume and flow rate of the lava, the eruption environment in which the flows are emplaced (subaerial, subaqueous, or subglacial), and the chemical composition (including gas and crystal contents) of the erupted lava (e.g., Zimbelman and Gregg, 2000). The majority of erupted lavas on Earth, as on other planets, is silicate, specifically *mafic* (magnesium- and iron-rich) in composition (e.g., BVSP, 1981). Typically, mafic lavas (i.e., basalts) tend to be relatively low in silica and alumina (<55% SiO<sub>2</sub>, <15% Al<sub>2</sub>O<sub>3</sub>; see e.g., McBirney, 1993) and relatively high in magnesia and iron (>5% MgO, >10% FeO<sub>tot</sub>). This results in relatively low-viscosity (50–300 Pa·s) fluid lava flows capable of long distance flow (tens to

hundreds of kilometers) given appropriate effusion rates and emplacement mechanisms (i.e., channels or tubes). Basalts, similar to those that erupt on Kilauea, Hawaii, and elsewhere in the Solar System, can have these characteristics for appropriate compositions, temperatures, and eruption rates. Another possible candidate material for Io's lavas are ultramafic lavas (e.g., komatiites), known to have erupted in the Precambrian, and thought to have had much higher magnesia contents (>18% MgO) and even lower viscosities (0.1–10 Pa·s: e.g., Huppert and Sparks, 1985), although the flow dimensions and emplacement styles of these lavas remain equivocal. More silica-rich, *felsic* lavas (andesites and rhyolites) are common on Earth, have higher dynamic viscosities (>500 Pa·s), and tend to produce relatively shorter, stubby, blocky flows and lava domes (e.g., Schmincke, 2004). Dacitic compositions have been identified recently by spectroscopy on Mars (Christensen *et al.*, 2005); however, andesitic and rhyolitic lavas have not been positively identified on any planet other than Earth, and will not be discussed further. In addition to these and other more rare silicate lavas, non-silicate lava flows have erupted on Earth, including carbonatites (carbonate-dominated lavas) and sulfur flows (important for Io). The nature of terrestrial sulfur flows will be discussed shortly.

In addition to lava composition (including volatile gas content (primarily H<sub>2</sub>O, CO<sub>2</sub>, SO<sub>2</sub>, H<sub>2</sub>S, and HCl) and the presence of various types of solids in the lava, which vary widely), the products and emplacement styles of terrestrial lavas are controlled by the environment in which they are emplaced. The term “environment” in this context includes not only the nature of the ground on which the lava flows (e.g., factors such as slope and confining topography, and composition, degree of consolidation, and volatile content of the substrate) but also the temperature and nature of the overlying material (air, water, or ice). Most studies of lava flows over the last two centuries have focused on understanding the emplacement dynamics of subaerial lava flows, using the active basaltic volcanoes of Mauna Loa and Kilauea (Hawaii) and Etna (Italy) as benchmarks (e.g., Rhodes and Lockwood, 1995; Heliker *et al.*, 2003; Bonaccorso *et al.*, 2004). More recently, the advent of research submersibles has allowed the study of submarine lava flows, and ongoing study of volcanoes in Iceland has led recently to focused research in volcano–ice interactions (e.g., Smellie and Chapman, 2002). Because our focus is in understanding effusive volcanism on Io from relatively low-resolution orbital spacecraft data (similar in context to aerial photographs and satellite imagery obtained of terrestrial flows), we will concentrate our discussion in this brief overview on the types and emplacement styles of subaerial terrestrial basalt lava flows.

In general, terrestrial basaltic flows are emplaced with two primary morphologies: pahoehoe and ‘a’a (e.g., Wentworth and Macdonald, 1953; block flows are a less common third type not discussed here). Pahoehoe flows tend to have smooth, ropy surfaces, whereas ‘a’a flows tend to have rough, fragmental surfaces (Hess and Poldervaart, 1967). Basaltic eruptions often start as pahoehoe and transition into ‘a’a downstream. Pahoehoe flows are typically fed by lava tubes in compound flow fields, which grow by budding of individual lobes at the distal end of the tube, and by inflation as fresh lava accumulates under a thin insulating crust (Hon *et al.*, 1994). ‘A’a flows are typically fed by open channel flow, often at higher effusion rates and over

steeper slopes than pahoehoe flows, and usually have higher gas contents than pahoehoe flows. These and other factors result in fragmentation of the lava into many small, clinkery pieces as cooling and crystallization proceeds (MacDonald, 1967). However, these descriptions are generalized, and it has proven difficult to disentangle all of the separate factors which control the emplacement of basaltic lava flows. In both cases cooling of the flows is dominated by radiative heat loss from their upper surfaces; a similar process occurs on Io, but is much greater due to the cold vacuum and thin transient atmosphere that is present there. When a basaltic magma chamber erupts its contents into an overlying confined depression, a lava lake can form. Such a feature is distinct from a ponded lava flow as long as the source of the lava in a lava lake can be continually replenished from the underlying chamber.

An important ongoing debate regards the emplacement style(s) of large-volume basaltic provinces, particularly continental flood basalts (CFBs). This is important for Io as large-volume flow fields akin to CFBs are clearly recognized in spacecraft images. CFBs, typified by the Columbia River Flood Basalt Province (e.g., Reidel and Hooper, 1989), are hundreds of kilometers long and contain tens to hundreds of individual flow units  $\sim 5\text{--}50$  m thick. Originally, these flow fields were hypothesized to form by rapid emplacement of thick, turbulent, high effusion rate lava eruptions over shallow ( $<1^\circ$ ) slopes (Shaw and Swanson, 1970). New studies suggest that at least some parts of several CFBs were slowly emplaced as initially thin, compound, inflationary pahoehoe flow fields (Self *et al.*, 1997). The potential role of rapid, perhaps turbulent, emplacement of lava flows has been of interest primarily in the study of Precambrian komatiite flows, as turbulent flow is a natural consequence of the inferred lava compositions and observed flow thicknesses of komatiites (Huppert and Sparks, 1985). However, recent work on terrestrial komatiites has found evidence for more Hawaiian-like compound emplacement at some localities (e.g., Cas and Beresford, 2001). Because no terrestrial ultramafic (komatiite) eruptions have ever been observed, their emplacement style(s) have been inferred from the chemical and physical properties of rock samples and study of the morphologies of metamorphosed and structurally disrupted Archean and Proterozoic outcrops (see e.g., Hill *et al.*, 1990, 2001). The role of emplacement styles of mafic and ultramafic lava flows in regards to Ionian eruptions will be discussed in later sections.

Effusive sulfur volcanism is rare on Earth, although yellow, fumerolic sulfur deposits are a common occurrence at many volcanoes (Banfield, 1954). Active sulfur lava flows have been observed at many volcanoes, including Siretoko-Iosan, Japan; Lastarria, Chile; Arenal and Poas, Costa Rica; and Vulcano, Italy, and sulfur flow deposits have been identified at many other volcanoes (see Kargel *et al.*, 1999 for a review). Terrestrial sulfur flows are thought to have formed from mobilization of remelted fumerolic sulfur deposits (Watanabe, 1940; Skinner, 1970), in which melting was induced by an adjacent heat source, either hot volcanic gases and/or hydrothermal waters (Watanabe, 1940; Oppenheimer, 1992) or intrusion of fresh silicate magma (Greeley *et al.*, 1984; Naranjo, 1985) on or near fumerolic sulfur deposits. Most sulfur flows are thought to be emplaced in a style similar to that of modern basaltic flows, as they have morphologies consisting of multi-lobed flows with surficial crusts, pahoehoe and 'a'a surface textures, and tubes and channels (Watanabe, 1940;

Greeley *et al.*, 1984; Naranjo, 1985). Harris *et al.* (2000) reported evidence for “self-combusting” sulfur flows at Vulcano, Italy, in which hot sulfur flows moving through topographic depressions thermally eroded solid sulfur in their substrates, leaving erosion trenches that were tens of centimeters wide and deep.

Unlike silicate lavas, sulfur lavas undergo dramatic color changes as they crystallize and interact with other materials. Understanding these color changes in sulfur is important in understanding volcanism on Io, as we see a wide range of colorful sulfur deposits in spacecraft images. On Earth, for example, the 1998 Vulcano self-combusting sulfur flows were yellow to moderate olive-brown (<120°C) in color and contained higher temperature (120–160°C) interior zones of dark red sulfur. This differs from the active flows of the 1936 Siretoko-Iosan eruption that were described as “chocolate brown”, and cooled to a yellow-green color (Watanabe, 1940). A solidified Mauna Loa sulfur flow was reported as yellow in color (Greeley *et al.*, 1984). Some of the color changes are due to the reorganization of sulfur molecules during cooling (Theilig, 1982), whereas other changes are due to small (<1 wt%) impurities (e.g., chalcophile elements, opaque crystals, carbonaceous or organic materials) in the lava (Kargel *et al.*, 1999). Even exposure to a vacuum induces color changes in sulfur, turning yellow, tan, and brown sulfur white within ~100 hours (Nash, 1987). Unmelted yellow sulfur powder brightens to a very light yellow/white-gray when exposed to radiation (see e.g., Steudel *et al.*, 1986; Nash, 1987). More work on terrestrial sulfur and sulfur flows is needed to better understand the role of sulfur color changes on Io’s surface appearance.

## 7.3 PREVIOUS WORK: INSIGHTS FROM VOYAGER AND TELESCOPIC STUDIES

### 7.3.1 Introduction: initial indications and discovery of volcanism

Our understanding of the nature of effusive eruptions on Io has changed considerably over time as *Voyager*, *Galileo*, and ground-based observations have refined the estimates of the temperature ranges involved, as higher spatial resolution observations have revealed morphological detail, and as both higher spatial resolution and a longer time base have revealed more fully the range of eruption types which occur.

Although ground-based observations were obtained in the 1970s, which in retrospect detected thermal emission from volcanic eruptions, they were not clearly recognized as such until 1979 when the first theoretical predictions of volcanism were made (Peale *et al.*, 1979) and *Voyager I* observed obvious evidence of plumes, volcanic surface features, and infrared emission (Morabito *et al.*, 1979; Smith *et al.*, 1979; Hanel *et al.*, 1979). With that evidence it became clear that the high in-eclipse infrared brightness observed earlier by Hanson (1973) and also by Morrison and Cruikshank (1973), and attributed to unusual thermal inertia values, was due at least in part to thermal emission from volcanic hot spots. The same was true for the infrared outburst observed by Witteborn *et al.* (1979) on 20 February

1978. In that observation, excess 4.0–5.4  $\mu\text{m}$  emission present for only one night had a spectrum roughly corresponding to a 600 K black body covering an area of 8,000  $\text{km}^2$ . Witteborn *et al.* had in fact discussed the possibility of volcanic activity in their paper but dismissed it as unlikely and concentrated on other possible explanations.

### 7.3.2 Early results from the *Voyager* observations: the sulfur vs. silicate controversy

The visible images and infrared spectra obtained by the *Voyager* spacecraft revealed clear evidence of effusive volcanism (summarized in Schaber, 1982), such as flow-like features radiating from central vents or the margins of paterae (volcano–tectonic depressions similar to calderas), albedo patterns thought to indicate lava lakes within paterae, and indirect evidence that various plains units might have been created by numerous flows. However, it remained unclear how much of that activity was directly due to silicate volcanism and how much was due to sulfur. Sulfur had been detected in the Jovian magnetosphere (Kupo *et al.*, 1976) and sulfur dioxide frost and gas had been recognized in ground-based spectra (Smythe *et al.*, 1979; Nash and Nelson, 1979; Fanale *et al.*, 1979) and spacecraft observations of the Loki region (Pearl *et al.*, 1979). The unusual color patterns present in regions such as Ra Patera (Pieri *et al.*, 1984) were also thought to be indicative of sulfur (perhaps quenched) in various stages of cooling (Section 7.2). However, the lack of spectral features or flow morphologies that could unambiguously be attributed to elemental sulfur led to continuing controversy regarding the relative importance of sulfur vs. silicate volcanism (Sagan, 1979; Young, 1984). Those in favor of predominately silicate volcanism argued that volatile sulfur and sulfur compounds simply acted as “paint” on a primarily silicate surface.

One argument against the presence of sulfur came from the observed strength of the lithosphere, as indicated by the presence of steep topography such as high patera walls (Clow and Carr, 1980). If temperature increased with depth at a rate implied by: (1) the high heat flow measured by Morrison and Telesco (1980), Matson *et al.* (1981), and Sinton (1981), coupled with (2) the commonly assumed conductive transport of that heat, then at shallow depths any sulfur would soften and produce too weak a lithosphere. Many Io researchers failed to appreciate the early arguments of O’Reilly and Davies (1981) that the very high resurfacing rates associated with predominately advective transport of heat via magma could in fact suppress the geothermal gradient to a value far below what would be implied by conductive transport, thus resulting in a cold lithosphere, strong even in the presence of sulfur.

On the other hand, part of an initial bias toward sulfur volcanism also resulted from an unfortunate wavelength gap in the *Voyager* instrumentation which made high-temperature silicate activity less obvious. The *Voyager* vidicon-based imager had filters covering the 0.35–0.62  $\mu\text{m}$  range while the IRIS spectrometer had little sensitivity shortward of 4  $\mu\text{m}$ . As a result, the high spatial resolution visible camera could not detect thermal emission while the relatively low spatial resolution infrared spectrometer saw emission almost completely dominated by the cooler but areally much larger portions of the hot spots. The center-of-gap wavelength of  $\sim 2 \mu\text{m}$  corresponds to the peak of the Planck black-body emission from a 1,500-K surface and therefore

*Voyager* was relatively insensitive to such surfaces. Typical analysis of *Voyager* infrared observations (Pearl and Sinton, 1982) consisted of few-component black-body models where the highest temperature components were less than or equal to  $\sim 650$  K – a value still attributable to sulfur. The consensus view did not begin to shift to silicate-dominated volcanism until two events occurred. First, in an early prescient paper Carr (1986) recognized that silicate flows cooled so quickly that their surfaces would also be dominated by low temperatures. Those type models were further developed by Davies (1996) and Howell (1997). Second, ground-based monitoring programs (discussed below) eventually detected outbursts still young enough to be dominated by high-temperature material too hot to be consistent with sulfur (Johnson *et al.*, 1988; Blaney *et al.*, 1995; Blaney *et al.*, 1997; Stansberry *et al.*, 1997).

### 7.3.3 Initial insights from the ground-based monitoring program

Several intensive ground-based monitoring programs began immediately after the *Voyager* discovery of volcanism provided an explanation for the previously anomalous infrared measurements. Most notable were the Hawaii group of Bill Sinton and coworkers (e.g., Sinton, 1980; Sinton *et al.*, 1980; Sinton, 1981; Sinton *et al.*, 1983) and the Jet Propulsion Laboratory (JPL) group (e.g., Matson *et al.*, 1981; Johnson *et al.*, 1984; Veeder *et al.*, 1994). Those initial observations provided wider spectral and temporal coverage than the brief *Voyager I* and *Voyager II* fly-bys, but with no spatial resolution beyond what could be gleaned from variations in the hemisphere-wide integrated flux. Eclipse observations by the above groups and others such as Morrison and Telesco (1980) provided the most direct way to separate hot spot emission from reflected and reradiated sunlight thus giving global heat-flow estimates, but the measurements were applicable only to the Jupiter-facing hemisphere. Monitoring of photometric variations due to Io's rotation could be used to locate in longitude particularly bright hot spots, and longer term observations could establish their stability and eruption lifetimes. Initial results indicated heat flow values in the range of  $1\text{--}2.5$   $\text{W m}^{-2}$ , higher than expected from the simplest steady-state tidal heating models (Yoder, 1979), thereby raising questions of whether non-equilibrium models or intermittent styles of activity were required. While infrared observations showed considerable variability, comparison of modern visible wavelength rotational light curves with those obtained decades earlier showed no detectable variation (Morrison *et al.*, 1979). This implied that despite the high ( $\geq 1$   $\text{mm yr}^{-1}$ ) resurfacing rates and the dramatic local albedo changes seen in the four short months between the *Voyager I* and *II* images, Io's surface somehow maintained persistent hemispheric albedo patterns.

### 7.3.4 Continuing analysis of *Voyager* observations

Continued analysis of *Voyager* data led to further insights regarding volcanic activity on Io. For example, McEwen and Soderblom (1983) recognized two types of volcanic plumes typified by the volcanoes Pele and Prometheus. The first was thought to be characterized by short eruption times of days to weeks, by plume heights of  $\sim 300$  km,

by sulfur lava vent temperatures of  $\sim 650$  K, and by dark plume deposits containing little  $\text{SO}_2$ . The second was thought to be characterized by lower temperature reservoirs with several year-long eruption times, plume heights from 60–100 km, and by ring deposits  $\sim 250$  km in diameter, rich in  $\text{SO}_2$ . *Galileo* results (see Chapter 8) have confirmed the existence of distinctly different plume types, but we now know the connection to underlying lava activity is different than originally assumed.

A comparison of *Voyager* imaging and infrared data led to the discovery (McEwen *et al.*, 1985) of a well-defined correlation between volcanic hot spots and low-albedo features. Most of the low-albedo features occurred on the floors of volcanic paterae. The correlation was ascribed to the absence of bright materials, such as  $\text{SO}_2$  frost, and the presence of a low-albedo substance. However, *Voyager* images did not provide enough spectral detail to uniquely determine the nature of the low-albedo material, and liquid sulfur, silicate–sulfur mixtures, and various other substances were all considered possible. The spectra did not appear consistent with pure silicates. The temperature distribution obtained, 200–400 K, was (once again partly due to wavelength gaps) consistent with liquid sulfur, but the presence of sulfur lava could not be determined conclusively.

### 7.3.5 Further development of ground-based observations: individual hot spots and silicate temperatures

During the 1980s various infrared techniques were developed providing sufficient spatial resolution to monitor thermal output from individual Ionian hot spots. These included speckle interferometry (Howell and McGinn, 1985; McLeod and McCarthy, 1991), polarimetry (Goguen and Sinton, 1985), Galilean satellite mutual occultation photometry (Goguen *et al.*, 1988; Medina *et al.*, 1989; Descamps *et al.*, 1992; Spencer *et al.*, 1994), Jupiter occultation photometry (Spencer *et al.*, 1990), and improvements in infrared cameras and telescope image quality such that hot spots could be directly resolved on the 1.2-arcsecond disk of Io (Spencer *et al.*, 1994). Continued monitoring also provided observations of unusual events, including an outburst in 1986 (Johnson *et al.*, 1988) which clearly had a temperature ( $\sim 900$  K) in the silicate range. Limited observations were also obtained with the NICMOS instrument on the Hubble Space Telescope (HST) (Goguen *et al.*, 1998). The observations showed continued although varying activity at major *Voyager*-era hot spots such as Loki and Pele, as well as surprisingly stable activity at newly discovered but fainter sources such as Kanehekili (Spencer *et al.*, 1990). The ground-based observation programs were intensified during the *Galileo* era (Howell *et al.*, 2001) to provide context for the more detailed but temporally isolated spacecraft observations. For example, they provided temporal constraints on the timing of the Tvashtar eruption seen by *Galileo*. They also enabled the recognition of patterns of activity such as the reoccurring brightenings seen at Loki.

Because Loki is the largest and often the brightest hot spot on Io it is also the best characterized, but the precise nature of the activity remains uncertain. Questions also exist concerning how representative this activity is of other smaller hot spots. The observations summarized in Rathbun *et al.* (2002) show that from 1988 through 2000

Loki brightened significantly every  $\sim 540$  days, with the bright period lasting approximately  $\sim 230$  days. As best as can be discerned from the limited *Galileo* observations, the brightenings correspond to a resurfacing wave that sweeps counterclockwise around the dark section of the patera. Rathbun *et al.*'s preferred interpretation is that the wave represents the foundering of the solid crust of a silicate lava lake (see Section 7.4.2), and the period represents the time required for new crust to thicken to the point where a density instability leads to overturn. Analysis and modeling of near-infrared mapping spectrometer (NIMS) data by Lopes *et al.* (2002) and Howell and Lopes (2004) is also consistent with the lava lake model. However, a comparison of Loki's activity with terrestrial lava lakes (Gregg and Lopes, 2004) reveals significant differences. Davies (2003) has produced thermal models of Loki, and believes the wave could also be consistent with spreading lava flows confined by patera walls. The situation became more complicated in 2000 when the semi-periodic behavior seemed to end and Loki entered an apparently more sustained but intermediate level of activity (Rathbun *et al.*, 2003).

#### 7.4 NEW INSIGHTS: GALILEO AT IO (1996–2001)

The *Galileo* mission to Jupiter afforded researchers the opportunity to obtain a wide range of data on Io's volcanoes, primarily from the solid-state imager (SSI), NIMS, and the photopolarimeter and radiometer (PPR). Not only did these instruments image Io at a wide range of resolutions covering various parts of the visible, near-infrared, and thermal-infrared portions of the electromagnetic spectrum, but also they imaged various parts of Io repeatedly during the course of the nominal and two extended missions (1996–2001). Having both varying spatial and temporal resolutions was instrumental in identifying many aspects of the styles of volcanic eruptions on Io. In this section, we discuss the new insights into effusive volcanism on Io garnered through these various SSI, NIMS, and PPR observations. To aid in the discussion we created a chart (Figure 7.1) to correlate inferred compositions of effusive products to eruption styles identified from repeated imaging.

##### 7.4.1 Composition of volcanic products

Insights into the chemical composition of volcanic products on Io was provided by analysis of SSI color data (Geissler *et al.*, 1999: 6 wavelengths: violet, green, red, 756 nm, 889 nm, 968 nm; see Klaasen *et al.*, 1984 for filter bandpasses) and NIMS spectroscopy (Carlson *et al.*, 1992; Smythe *et al.*, 1995: coverage of the 1–5.2- $\mu\text{m}$  range with resolution of 0.025  $\mu\text{m}$ ), as well as data from HST (Spencer *et al.*, 2000a). Basically, Io can be subdivided into four main color units: yellow, gray–white, black, and red. The yellow unit covers about 40% of Io's surface (Geissler *et al.*, 1999) as large expanses of equatorial plains, with more localized greenish-yellow patches observed in some paterae. Geissler *et al.*'s (1999) comparison of *Galileo* SSI color data to the laboratory spectra of >650 rocks and minerals suggested

VOLCANISM ON IO				
Inferred Lava Composition (based on SSI color and NIMS spectroscopy)				
Inferred Eruption Style (based on repeated SSI, NIMS, & PPR imaging)	Black (Silicate-dominated)		Yellow (Sulfur-dominated)	White (SO <sub>2</sub> -dominated)
	Explosion-dominated (Short duration, energetic events, very high brightness temperatures)	Pillan, Thor, Tvashtar (Rapidly-emplaced, possibly turbulent, mafic to ultramafic flows)	Ra flow field ? (Large-volume, bright, flow-like deposits associated with dramatic event, 1994-95)	None detected
	Intra-Patera (Variable durations, activity confined in paterae, variable brightness temperatures)	Loki, Pele, Tapan patera floors (Lava lakes, mafic to ultramafic flows)	None detected	None detected
	Flow-dominated (Long duration, continuous output, high brightness temperatures)	Prometheus, Amirani (Slowly-emplaced, compound inflationary mafic flows)	None detected	None detected
	Unnamed (Short duration, weak event, low brightness temperatures)	X	Tsui Goab Fluctus (Small-volume, inflationary sulfur flow)	None detected
	Unidentified (Unknown eruption style)	X	X	Balder, Tohil (Glacial-like flow?)

Figure 7.1. Chart relating volcanism on Io to inferred composition of volcanic products and eruption styles, emphasizing emplacement of effusive materials.

that the yellow materials were most consistent with cyclo-octal sulfur (S<sub>8</sub>) with or without a covering of SO<sub>2</sub> frosts deposited by plumes. Alternatively, Hapke (1989) hypothesized that the yellow color on Io could be produced by polysulfur oxide and S<sub>2</sub>O without requiring large quantities of elemental sulfur. The rare greenish-yellow patches on some patera floors were suggested by Geissler *et al.* (1999) to be composed either of some type of sulfur compound contaminated by iron, or lava flows composed of silicates rich in olivine or pyroxene with or without sulfur-bearing contaminants. Geissler *et al.*'s interpretations of the "green spots" suggest intimate interaction between silicate lava and either sulfurous flows or plume deposits (see also McEwen *et al.*, 2000; Williams *et al.*, 2000a).

The gray–white color unit covers about 27% of Io's surface (Geissler *et al.*, 1999) as extensive equatorial plains and as diffuse rings around active vents, and has been thought to be dominated by solid sulfur dioxide. This unit was extensively studied by NIMS, which observed several different strength bands of SO<sub>2</sub> that could be analyzed to assess grain size and abundance (e.g., Douté *et al.*, 2001, 2002, 2004). The white unit was found to be mostly coarse- to moderate-grained SO<sub>2</sub> snow (Carlson *et al.*, 1997), likely resulting from plume fallout that has undergone recrystallization (Douté *et al.*,

2001, 2002). However, high spatial resolution NIMS data showed that color alone is not in itself a good indicator to map SO<sub>2</sub> distribution or granularity (pure SO<sub>2</sub> is transparent in visible light), suggesting that the SO<sub>2</sub> in the gray–white color unit is often mixed with other contaminants, especially where strong NIMS signatures of SO<sub>2</sub> coincide with non-gray–white materials (e.g., Lopes-Gautier *et al.*, 2000; Douté *et al.*, 2002, 2004).

The black color unit covers about 1.4% of the surface (Geissler *et al.*, 1999) and is mostly restricted to very dark patera floors, lava flow fields, or dark diffuse materials near or surrounding active vents, which correlate with active or recently active hot spots (Lopes-Gautier *et al.*, 1999, 2000; Lopes *et al.*, 2001). *Galileo* multicolor studies of the black materials (Geissler *et al.*, 1999) found that their visible/near-IR spectra were most consistent with Mg-rich orthopyroxene (enstatite or bronzite/hypersthene), as indicated by their strong 0.9- $\mu\text{m}$  absorption. The dark materials are hypothesized to be silicate lava flows (within flow fields), or lava lakes (within paterae), or pyroclastic deposits (within diffuse deposits near paterae), of mafic to ultramafic composition.

The red color unit is found either as local red patches and rings on or around some active vents (e.g., Pele), or as regional red–orange units in polar regions. The red has been interpreted to come from short-chain sulfur molecules (S<sub>3</sub>, S<sub>4</sub>) that result, in the case of the red patches and rings, from condensation and recrystallization of S<sub>2</sub>-rich volcanic gases in the plumes of active vents (Spencer *et al.*, 2000a). These short-chain sulfur molecules are probably ephemeral in nature (reverting back to yellow, long-chain S<sub>8</sub> upon cooling), and thus require continual replenishment to be observed. The more maroon–red polar units result from breakdown of cyclo-octal sulfur (S<sub>8</sub>) by charged particle irradiation (Johnson, 1997). Alternatively, recent studies of *Galileo* NIMS spectra of the red diffuse deposit south of Marduk combined with laboratory analyses suggest that at least some red deposits on Io result from solid sulfuryl chloride (Cl<sub>2</sub>SO<sub>2</sub>) or sulfur dichloride (Cl<sub>2</sub>S) that condensed on SO<sub>2</sub> snow from Cl-bearing gases in active plumes (Schmitt and Rodriguez, 2003).

In summary, the various compositional analyses during the *Galileo* era, using SSI color data and NIMS spectroscopy, supplemented by HST and other data (e.g., Spencer *et al.*, 2000a), has led to the tentative identification of at least three distinct volcanic compositions on Io: silicate, sulfur, and sulfur dioxide, although gaseous SO<sub>2</sub> in volcanic plumes was identified during the *Voyager* fly-bys (Pearl *et al.*, 1979). As we shall see, these three materials occur in a variety of morphologies and are combined in various ways through Io's active volcanic processes.

#### 7.4.2 Eruption styles

One of the primary advantages of repeated imaging of the anti-Jovian hemisphere during the *Galileo* mission was obtaining the potential to catch volcanoes in various parts of their eruption cycles, to identify both the *types* of eruptions occurring, and how those eruptions *evolved*. Through correlation of the SSI, NIMS, and PPR observations during each orbital fly-by with those of previous fly-bys, a set of three primary types of eruption styles were identified: flow-dominated volcanism

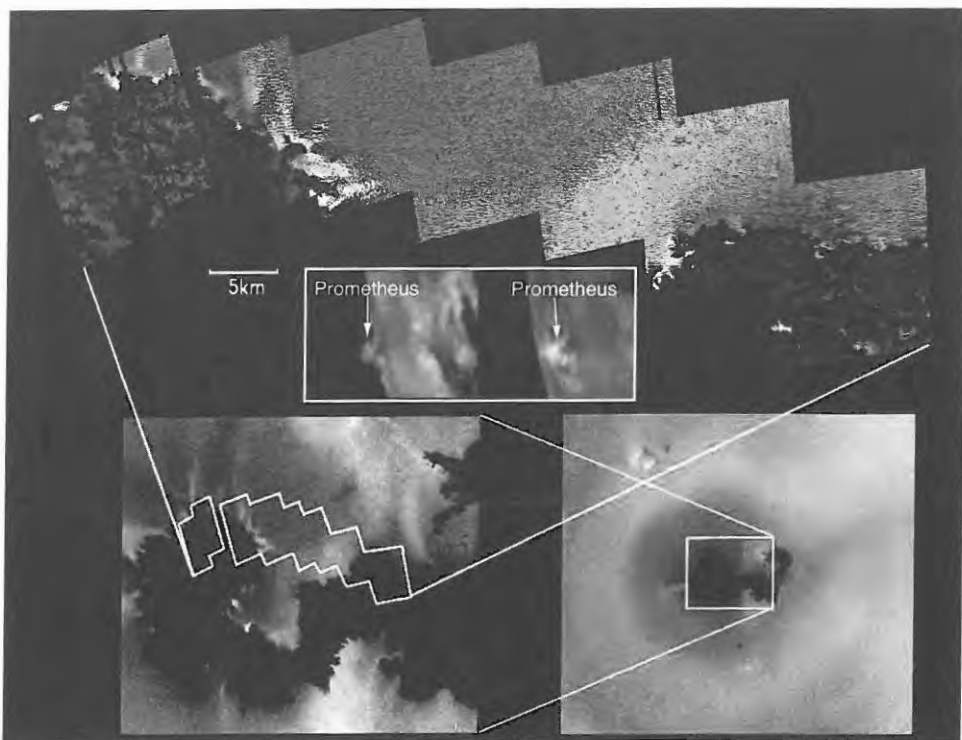


**Figure 7.2.** A montage of *Galileo* SSI images of the Prometheus volcano at several different resolutions, which identify various aspects of the flow-dominated eruption style. These eruptions produce compound silicate flow fields that are slowly emplaced over months to years, with measured temperatures consistent with terrestrial basaltic volcanism (Keszthelyi *et al.*, 2001). Note the small dark patches in the flow field indicative of recent breakouts. Heat from advancing flows vaporize  $\text{SO}_2$  snow producing jet-like flow front plumes (Kieffer *et al.*, 2000; Milazzo *et al.*, 2001). The central inset shows examples of the Prometheus plume. (See also color section.)

(formerly Promethean), explosion-dominated volcanism (formerly Pillanian), and intra-Patera volcanism (formerly Lokian). A previous designation system of these styles using the names of specific Ionian volcanoes was abandoned by mutual consent of Io researchers at the 2005 Io Workshop.

*Flow-dominated* (formerly Promethean) eruptions (Keszthelyi *et al.*, 2001), typified by eruptions at the Ionian volcanoes Prometheus (Figure 7.2) and Amirani (Figure 7.3), originate from either paterae or fissures, and produce extensive compound lava flow fields through repeated small breakouts of lava, similar to the slowly emplaced (months to years), compound inflationary flow fields in Hawaii. NIMS temperature measurements at these sites are consistent with temperatures associated with terrestrial basaltic volcanism. These eruptions are long-lived, steady eruptions that can last years at a time, and often include small (<200 km high) explosive plumes of vaporized sulfurous country materials

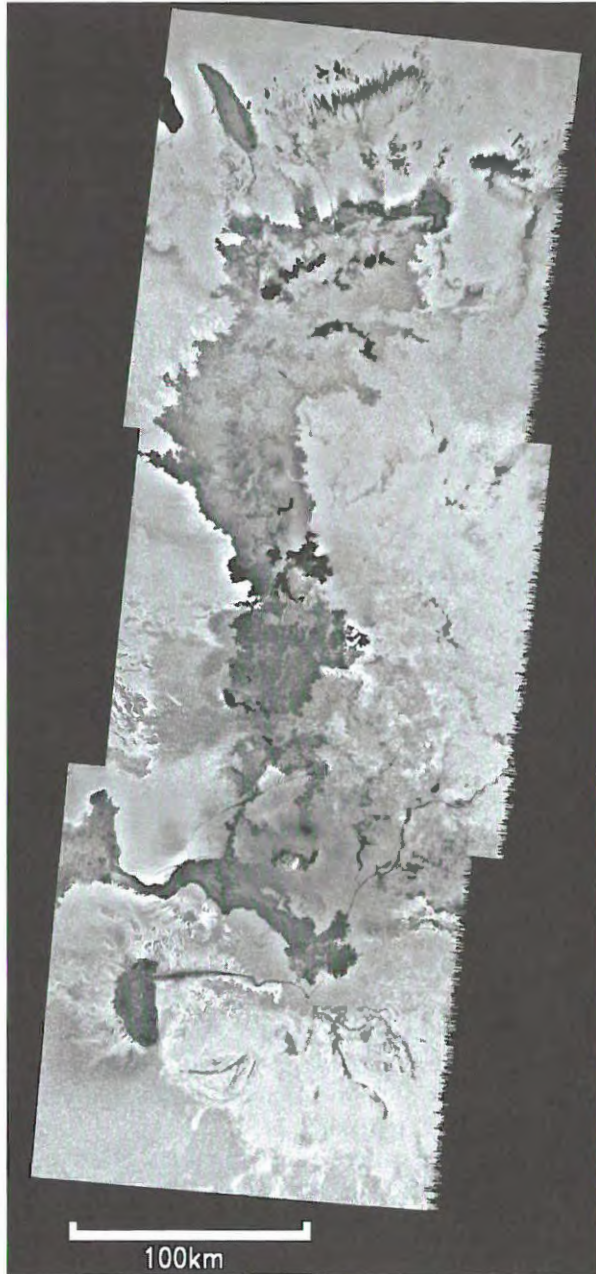


**Figure 7.3.** The Amirani flow field, as imaged by the *Galileo* SSI in February 2000. Amirani, like Prometheus, is an example of a flow-dominated eruption style, with dark lava flows slowly emplaced over many years (note the freshest, darkest flows near the top of the field). Presumably tube-fed lavas from southern Amirani are thought to feed the Maui flow field (off the image at bottom left) through a >300 km long active tube system, the longest known in the Solar System.

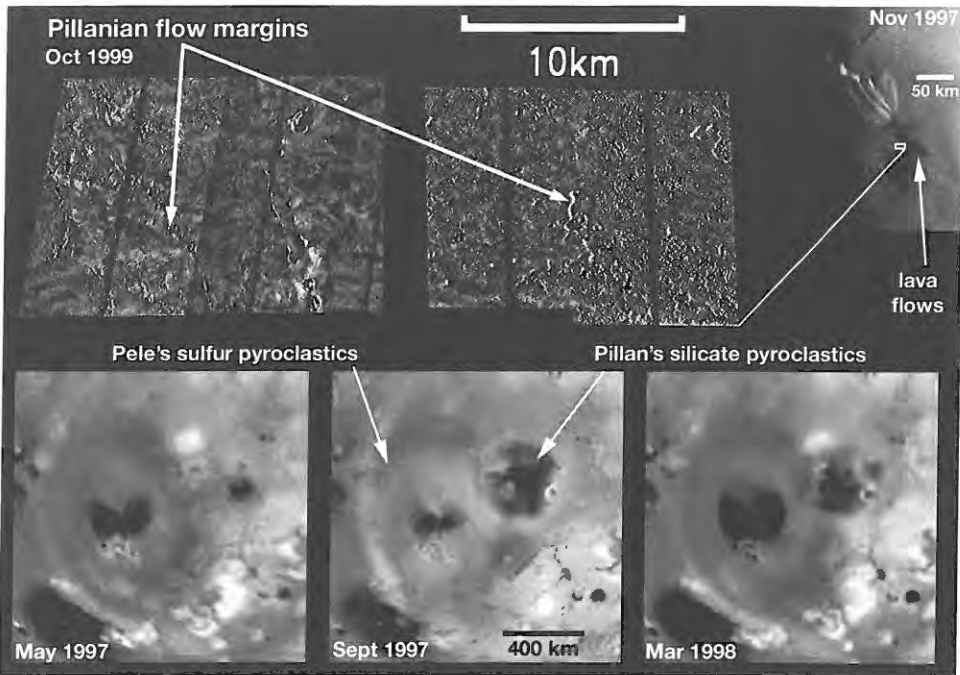


**Figure 7.4.** A montage of *Galileo* SSI images of the Pillan volcano at several different resolutions, which identify various aspects of an explosion-dominated (formerly Pillanian) eruption style. (*top*) The Pillan lava flow field, which emanated from fissures that fracture a mountain north of the caldera. (*bottom*) Changes to Pillan's surroundings (including Pele's red ring) due to activity at these volcanoes. These eruptions produce extensive flow fields that are rapidly emplaced over days to weeks, with measured temperatures consistent with terrestrial mafic to ultramafic volcanism (Keszthelyi *et al.*, 2001). (See also color section.)

that erupt from the edges of flow fronts (Kieffer *et al.*, 2000; Milazzo *et al.*, 2001), somewhat similar to the rootless conduits found in pahoehoe flow fields fed by lava tubes. The plumes associated with flow-dominated eruptions appear to be dominantly  $\text{SO}_2$  gas formed as the hot lava vaporizes  $\text{SO}_2$  snow on the plains, though ephemeral accumulations of diffuse red material (usually near the primary hot spot) may suggest the presence of  $\text{S}_2$  gas in some areas. The vaporized  $\text{SO}_2$  quickly refreezes and forms bright jets perpendicular to the flow front margins (Figure 7.2). The location of the plume source changes as the flow field slowly advances, which for the case of Prometheus covered a distance of 75–95 km between *Voyager* (1979) and initial *Galileo* observations (1996). Higher resolution *Galileo* SSI observations of equivalent resolution but separated by  $\sim 3$  months clearly show fresh breakouts of lava in the Prometheus and Amirani flow fields, similar in morphology to those seen in aerial photographs of the Pu'u' O'o'-Kupaianaha flow field, Kilauea Volcano, Hawaii (Keszthelyi *et al.*, 2001).

*Explosion-dominated* (formerly Pillanian) eruptions (Keszthelyi *et al.*, 2001), typified by some eruptions observed at the Pillan (Figure 7.4), Tvashtar

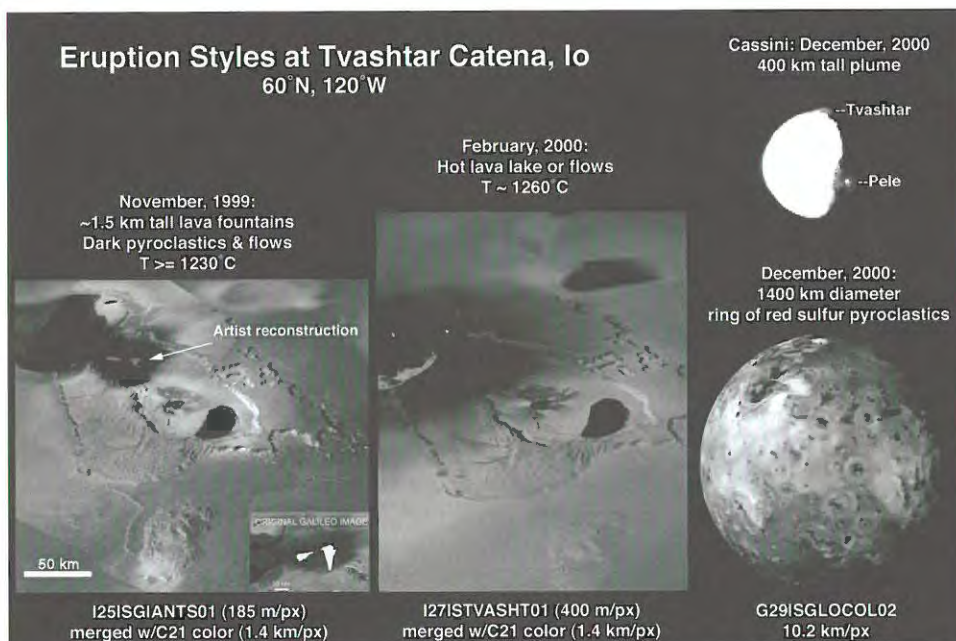


**Figure 7.5.** A montage of *Galileo* SSI and *Cassini* imaging science subsystem (ISS) images showing a range of eruption styles at Tvashtar. In November 1999 Tvashtar had a possibly flow-dominated eruption, producing a lava fountain and flow field. In February 2000 an intra-Patera eruption could have occurred, producing fresh material in a lava lake (or possibly just a confined lava flow). In December 2000, the *Cassini* spacecraft recorded an explosion-dominated eruption, from which *Galileo* imaged a large red ring deposit of sulfur. It remains unclear whether any new flows were emplaced (rapidly or otherwise) after the December 2000 event. (See also color section.)

(Figure 7.5), Surt, and Pele Volcanoes, also originate from either paterae or fissures. However, these eruptions differ from flow-dominated eruptions in that most of the energy of the eruption is directed into a short-lived, vigorous event that lasts days to weeks. These eruptions are discrete events compared with the more or less continuous flow-dominated eruptions like those at Prometheus. These eruptions produce both extensive pyroclastic deposits and dark lava flow fields. Temperatures associated with terrestrial mafic to ultramafic volcanism are correlated with these events. Explosion-dominated eruptions typically include large (>200 km high) explosive plumes, which occur due to the interaction of silicate magma with either juvenile or meteoric sulfurous volatiles. This most often results in large (~1,200 km diameter) red rings of short-chain sulfur around the source regions. However, the summer 1997 eruption at Pillan produced a ~400 km diameter dark diffuse deposit of silicate material, along with the highest temperatures recorded by the SSI and NIMS (~1,550°C: McEwen *et al.*, 1998b; ~1,600°C: Davies *et al.*, 2001). These temperatures, along with the identification of silicates in the black materials on Io (Geissler *et al.*, 1999),

suggested that either ultramafic or superheated basaltic volcanism was occurring on Io (McEwen *et al.*, 1998b; Kargel *et al.*, 2003). However, recent re-evaluation of the *Galileo* data and additional modeling of temperature fits to these data suggest that temperatures associated with these explosion-dominated eruptions may be more consistent with less ultramafic compositions ( $T \sim 1,200\text{--}1,300^\circ\text{C}$ ), more like those theorized for lunar mare basalts or terrestrial komatiitic basalts (see also Williams *et al.*, 2000b).

In terms of effusive products, explosion-dominated eruptions often produce areally extensive flow fields, but over a shorter eruption duration than the flow-dominated eruptions. For example, an  $\sim 3,100\text{-km}^2$  flow field formed between 52–167 days during the summer 1997 eruption at Pillan (Williams *et al.*, 2001a). The calculated volumetric flow rate for these lavas is  $\sim 1,740\text{--}7,450\text{ m}^3\text{ s}^{-1}$ , similar to the flow rates for the 1783 Laki eruption and theorized for the Rosa member of the Columbia River Flood Basalt (Thordarson and Self, 1993, 1998), but far above those for typical Hawaiian flows. The morphology of the Pillan lava flows, as imaged at  $\sim 20\text{--}30\text{ m}$  per pixel by the *Galileo* SSI in October 1999, shows an exceptionally rough, disrupted and platy upper surface, that was suggested to result from rapidly emplaced flows (Williams *et al.*, 2001a). Whether highly ultramafic compositions or turbulent lava flow are components of the emplacement of these flow fields cannot be assessed at present. However, it is clear that flow fields associated with explosion-dominated eruptions tend to be more rapidly emplaced than those associated with flow-dominated eruptions. At this point it is important to note, however, that many Ionian volcanoes produce both flow-dominated and explosion-dominated eruptions. For example, the *Galileo* spacecraft detected components of both flow-dominated and explosion-dominated eruptions at the Tvashtar Volcano during close fly-bys between 1999–2001 (Keszthelyi *et al.*, 2001; Turtle *et al.*, 2004; Milazzo *et al.*, 2005).

*Intra-Patera* (formerly Lokian) eruptions (Lopes *et al.*, 2004) are confined within paterae, or volcano–tectonic depressions similar to terrestrial calderas found in great number across Io's surface, ranging in size from 2–202 km diameter. These eruptions occur with or without associated plumes, and often erupt as lava lakes, some of which undergo occasional overturning or resurfacing of their upper solid crusts. The volcanoes of Loki (Io's most powerful volcano: Figure 7.6), Pele, Emakong (Figure 7.7), and Tupan (Figure 7.8) are all thought to produce this eruption style, though Pele also produces explosion-dominated eruptions (Lopes *et al.*, 2001; Radebaugh *et al.*, 2001, 2004). Combined Earth-based telescopic and *Galileo* PPR monitoring over many years led to the detection of reoccurring, almost periodic brightenings at Loki that have been interpreted as repeated foundering and growth of the crust of a lava lake on the floor of the Loki caldera (Spencer *et al.*, 2000b; Rathbun *et al.*, 2002; see also Section 7.3.5). The margins of these paterae are usually bright in NIMS images, indicating hot edges that are consistent with terrestrial lava lakes. Most of Io's active volcanoes, as identified by NIMS hot spots, coincide with these paterae, suggesting that most lava resurfacing on Io is confined within paterae, and that the high resurfacing rates on Io as a whole are dominated by plume eruptions and their deposits (Lopes *et al.*, 2004).

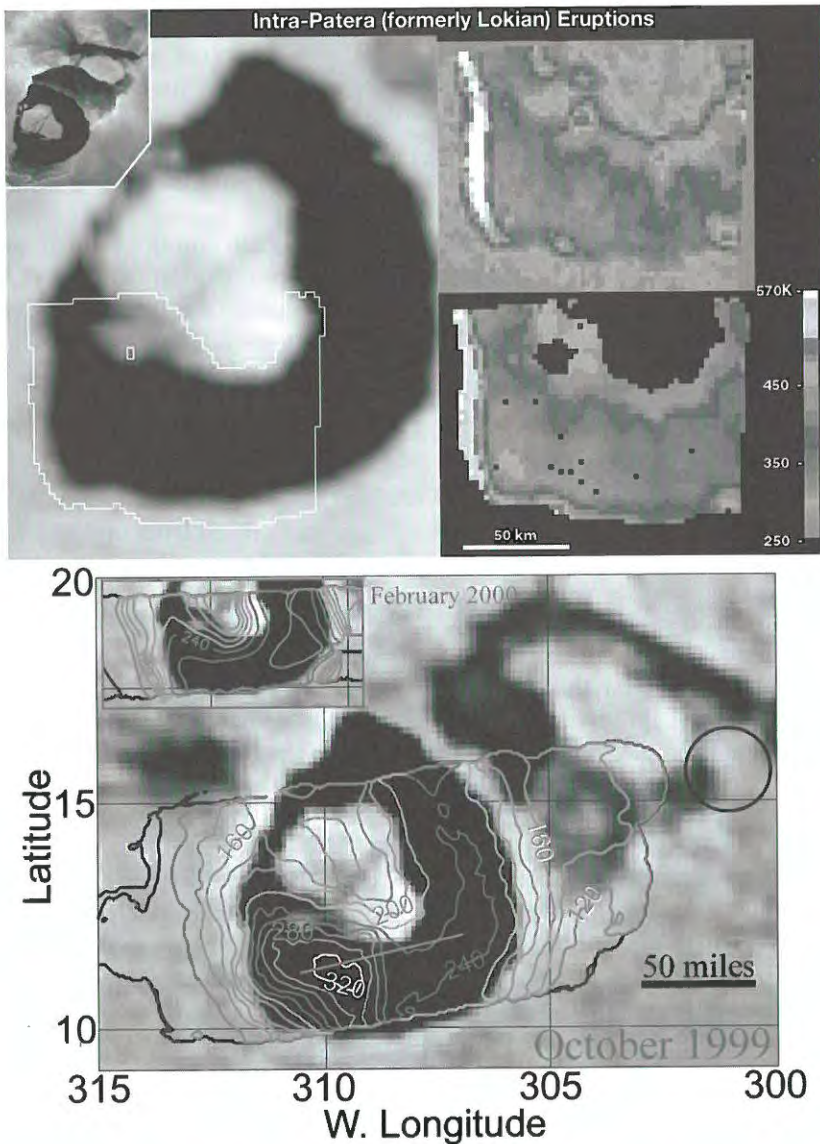


**Figure 7.6.** A montage of *Voyager* and *Galileo* SSI, NIMS, and PPR images of Loki volcano at several different resolutions and times, which identify various aspects of an intra-Patera (formerly Lokian) eruption style. These eruptions produce lava lakes that are overturned over months to years, with measured temperatures typically consistent with terrestrial basaltic volcanism (Lopes *et al.*, 2004). The color panel at upper right (see color section) is a NIMS map at  $2.5\ \mu\text{m}$  showing a hot edge (white:  $T \sim 840\ \text{K}$ ) at the western wall, whereas the image at lower right is a NIMS temperature map showing warmer and cooler parts of the patera floor. The bottom image shows PPR data over an image of Loki, showing the migration of the hottest part of the patera floor from west to east (from Spencer *et al.*, 2000b).

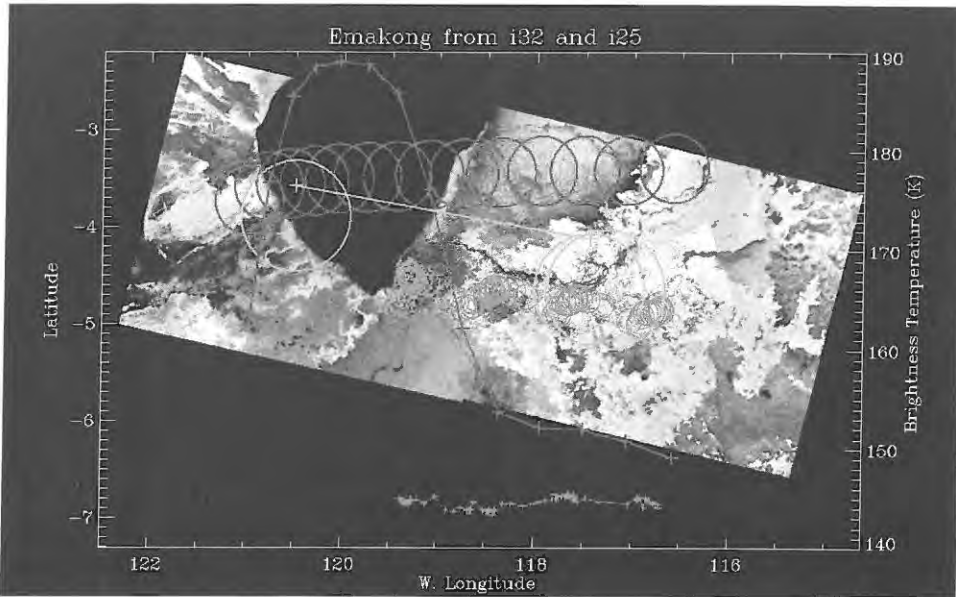


**Figure 7.7.** *Galileo* PPR data superposed upon SSI images of Emakong Patera. The PPR data demonstrates the very cold surface of the floor of Emakong Patera and its surrounding bright flows. NIMS data also showed that  $\text{SO}_2$  frost is stable on parts of the patera floor, which suggests that Emakong may represent a cooled, inactive sulfur volcano (or alternatively, a very cooled silicate volcano with silicate flows heavily mantled by sulfurous deposits: Williams *et al.*, 2001b). (See also color section.)

Some paterae (e.g., Loki, Tupan) have bright “islands” in their interiors that are partially or completely surrounded by the inferred lava lakes. How these cold islands are maintained for years when hot lava sources are adjacent is a mystery. In the case of Tupan (Figure 7.8), heat from the lava lake appears to melt bright sulfur deposits along the margins of the lake, which accumulate as bright “puddles” on the dark surface. Diffuse red deposits, presumably short-chain sulfur crystallized from  $\text{S}_2$  gas, cover the margins of the patera and large parts of the central island. NIMS temperature estimates for active paterae typically fall in the range consistent with terrestrial basaltic to ultramafic volcanism (Lopes *et al.*, 2001, 2004; Radebaugh *et al.*, 2004), although PPR observations show that the dark surface of Emakong Patera is very cold (Figure 7.7); NIMS also showed that  $\text{SO}_2$  is stable on the dark surface in some areas, and might represent an inactive, solidified sulfur lava lake.

### 7.4.3 Styles of non-silicate flow emplacement

Most sulfur and  $\text{SO}_2$  volcanism on Io is thought to be *secondary* (i.e., due to remelting and mobilization of crustal sulfurous materials by adjacent silicate heat sources), as originally suggested from *Voyager*-era studies by Greeley *et al.* (1984). Examples

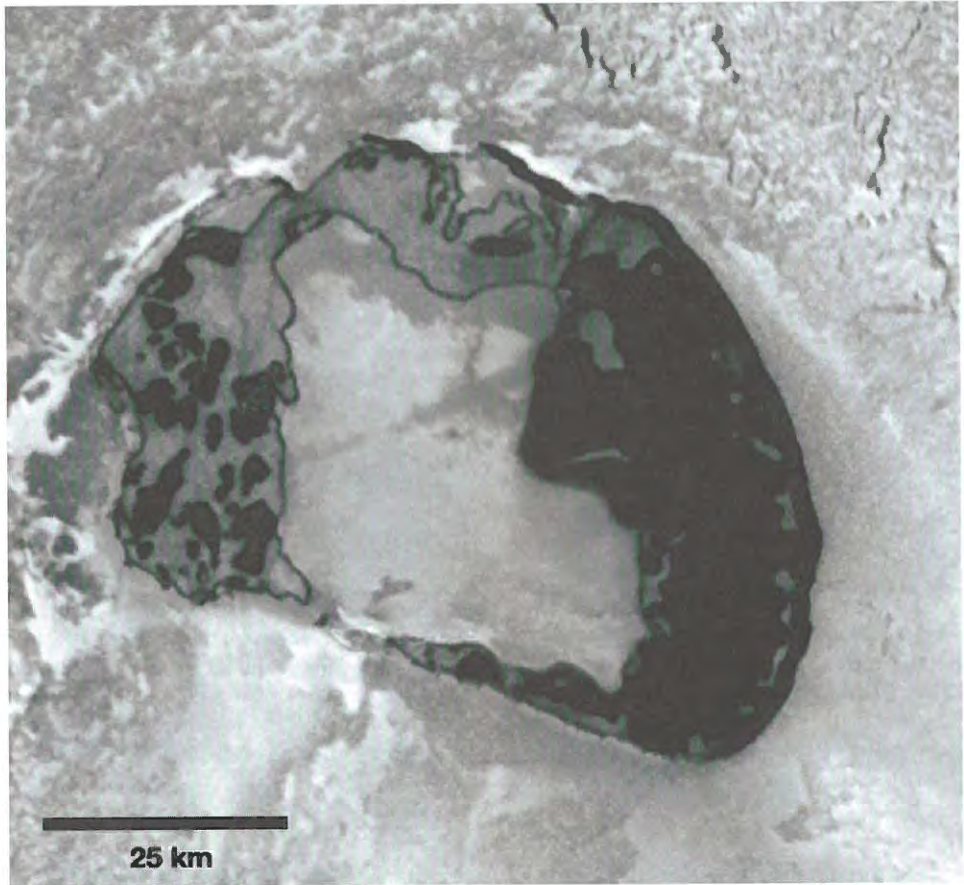


**Figure 7.8.** *Galileo* SSI image of Tupa Patera obtained in October 2001, another example of an intra-Patera eruption style. Heat from the lava lake appears to melt bright sulfur deposits along the margins of the lake, which accumulate as bright “puddles” on the dark surface of the lake. Diffuse red deposits, presumably short-chain sulfur crystallized from  $S_2$  gas, cover the margins of the patera and large parts of the central island. This is the highest resolution color image of Io obtained during the *Galileo* mission (132 m per pixel). (See also color section.)

include bright lava flows surrounding smaller volume dark flows at Sobo Fluctus in the Chaac–Camaxtli region (Williams *et al.*, 2002), and white (presumably  $SO_2$ -rich) flow front plumes jetting normal to the flow margins of the Prometheus flow field (Kieffer *et al.*, 2000; Milazzo *et al.*, 2001). During the *Galileo* era there was limited evidence for primary sulfur volcanism (i.e., not associated with nearby silicates). In 1994–1995, prior to *Galileo*’s arrival at Jupiter, there was a dramatic brightening detected by HST at the Ra Patera Volcano (Spencer *et al.*, 1997), and subsequent imaging by SSI showed clear surface changes in the form of bright, flow-like deposits of large areal extent (McEwen *et al.*, 1998a). *Voyager*-era studies of Ra Patera

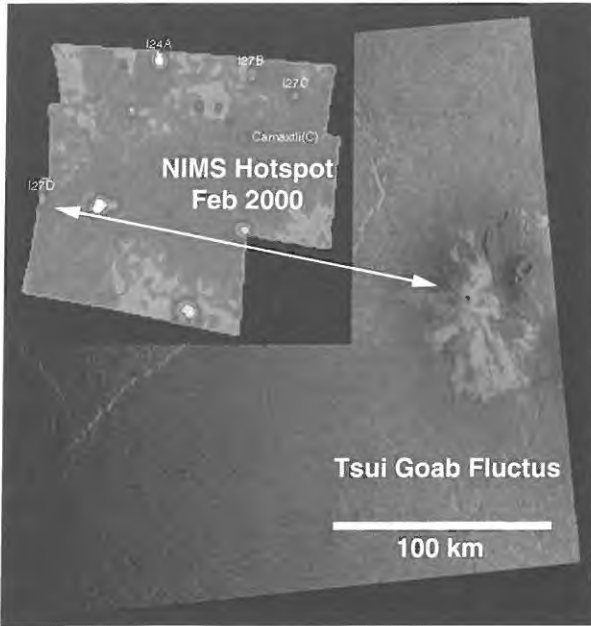


**Figure 7.9.** Low-resolution NIMS hot spot image (*inset*), with white arrows showing the correlation of the I27D hot spot of Lopes *et al.* (2001) with the bright flow field of Tsui Goab Fluctus in the Culann-Tohil region as imaged by the SSI during October 2001. This is the only location of potentially active, primary sulfur effusive volcanism detected during the *Galileo* mission. (See also color section.)

suggested it was a likely site for sulfur volcanism (Pieri *et al.*, 1984), and if the correlation between bright yellow materials and sulfur holds true, then the 1994–1995 event at Ra may be an example of an explosion-dominated style eruption including sulfur flows. However, no repetition of such an event has since been detected, either by *Galileo*, HST, or Earth-based telescopes.

An ~290 km long, yellow and white–gray flow extends north-east from the dark caldera-like Emakong Patera, which Williams *et al.* (2001b) suggested might be part of a large primary or secondary sulfur flow field making up the Bosphorus Regio area of Io. Although the colors of the Emakong flows match those of sulfur that has undergone radiation exposure (e.g., Nash, 1987), and the flow is fed by a dark curvilinear channel (consistent with hot sulfur), no surface changes were detected at Emakong during the *Galileo* mission. The best evidence for active sulfur volcanism occurred during the February 2000 fly-by, when NIMS detected a weak hot spot at Tsui Goab Fluctus (Figure 7.9), a bright flow field adjacent to an apparently inactive small shield volcano in the Culann–Tohil region (Williams *et al.*, 2004). The temperature measured by NIMS ( $\sim 260 \pm 95^\circ\text{C}$ ) falls with the range of molten sulfur, and there is no indication of any adjacent silicate volcanic activity. However, there was no evidence of surface changes in Tsui Goab Fluctus after the February 2000 event (SSI

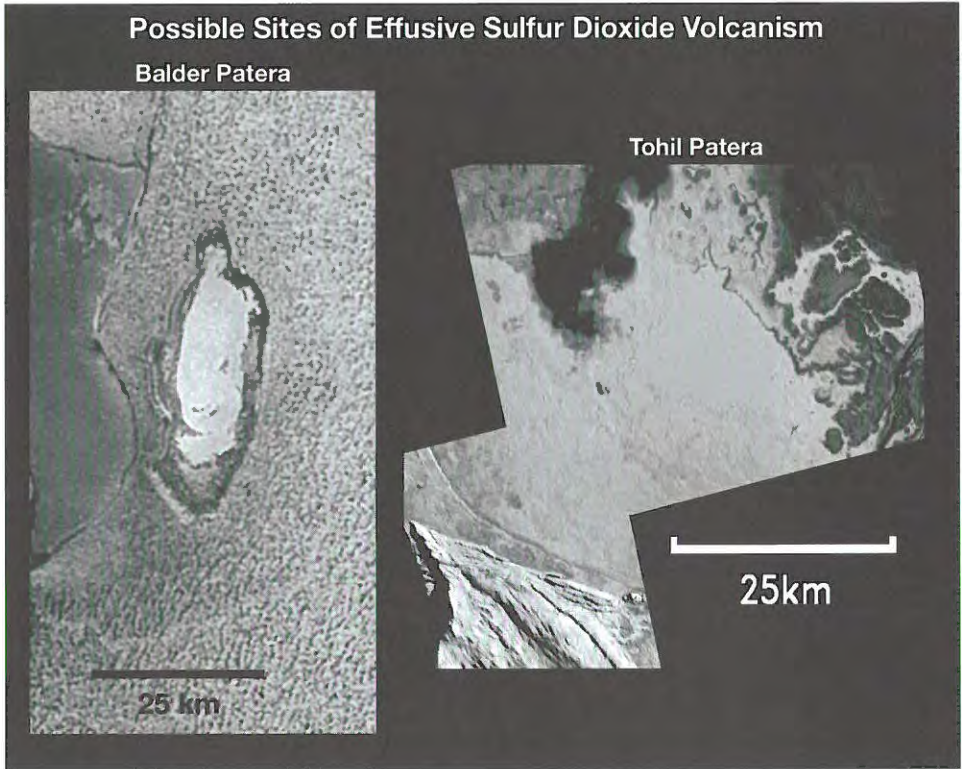


**Figure 7.10.** *Galileo* SSI images showing possible sites of effusive  $\text{SO}_2$  volcanism on Io. (*left*) Balder Patera in the Chaac–Camaxtli region (Williams *et al.*, 2002), site of a proposed glacial-like flow (Smythe *et al.*, 2000). (*right*) Tohil Patera in the Culann–Tohil region (Williams *et al.*, 2004), the south-west section of which has an enhanced  $\text{SO}_2$  signature and flow-like margins in its interior. (See also color section.)

coverage was of low-resolution), so if fresh sulfur flows were emplaced, they did not cover any new terrain.

Evidence for effusive  $\text{SO}_2$  volcanism is scant; most surface changes that show variations in  $\text{SO}_2$  content resolvable by NIMS are in the form of regional variations in the plains (Douté *et al.*, 2001, 2002, 2004), which are likely due to redistribution and/or recrystallization of explosively emplaced  $\text{SO}_2$  snow produced by freezing of volcanic gases (Carlson *et al.*, 1997). However, NIMS detected a strong signature of  $\text{SO}_2$  confined to the floor of Balder Patera in the Chaac–Camaxtli region (Williams *et al.*, 2002), which SSI shows to have a homogeneous white-colored patera floor (Figure 7.10). It is unclear why the floor should be so enriched in  $\text{SO}_2$  relative to the surrounding plains. Smythe *et al.* (2000) proposed that an  $\text{SO}_2$  glacial-like flow may have erupted and flooded the patera floor. Although the dynamics of such a flow have not yet been explored, mapping in the Culann–Tohil region has detected another

region of possible effusive SO<sub>2</sub> material. The south-east section of Tohil Patera contains a white material in which high-resolution SSI images show apparent flow margins (Williams *et al.*, 2004); NIMS indicates that this region also has a signature of enhanced SO<sub>2</sub>, although not as abundant as that at Balder Patera. Although these images are intriguing, additional assessment of the potential for SO<sub>2</sub> flows must await further study.

#### 7.4.4 Volcano distribution

Volcanoes on Io (and for that matter, the mountains too) do not appear to follow a distinct global pattern, suggesting that any surface expression of internal dynamics (convection) is subtle. Active hot spots appear to be randomly distributed (Lopes-Gautier *et al.*, 1999). The distribution of mountains and paterae (including those which have not been observed to be active) is, however, not random, as both types of features are concentrated toward lower latitudes and follow a bimodal distribution with longitude (based on available imagery). The greatest frequency of mountains occurs in two large antipodal regions near the equator at about 65° and 265° (Schenk *et al.*, 2001). In contrast, the volcanic patera follow a similar distribution but 90° out of phase with that of the mountains (Radebaugh *et al.*, 2001). The bimodal distribution pattern for paterae and other volcanic centers matches the expected pattern of heat flow from asthenospheric tidal heating (Ross *et al.*, 1990) and the pattern of internal convection within the mantle predicted from simulations (Tackley *et al.*, 2001). Jaeger *et al.* (2003) found that 41% of tectonically derived mountains are associated with paterae, and suggested that orogenic faults on Io act as conduits for magma ascent, fueling patera formation near mountains (see Chapter 6).

## 7.5 SUMMARY AND OUTSTANDING QUESTIONS

With the end of the *Galileo* mission, future studies of Io will rely upon the increasingly sophisticated observations possible from newly developed techniques at large ground-based observatories. Advanced speckle techniques (Marchis *et al.*, 2000, 2001) and adaptive optics systems (Marchis *et al.*, 2002; de Pater, 2004) are now producing infrared images of Io comparable with those obtained by the *Galileo* NIMS instrument during the early (non-Io-targeted) fly-bys. These techniques are also now being combined with spectral observations beyond the instrument capabilities of *Galileo*. These types of observations will enable us to address several outstanding questions regarding the nature of activity on Io. For example, the existing eruption record suggests there may be a change in eruption style with latitude, with larger, more violent, but less frequent eruptions dominating at high latitudes. However, the current statistics are insufficient to firmly conclude this. Another outstanding question is the presence of ultramafic temperatures above the liquidus temperature of basalt. These were detected during, for example, the 1997 Pillan eruption (McEwen *et al.*, 1998b), but recent reanalyses of *Galileo* data cast the occurrence of ultramafic temperatures in doubt (A. G. Davies and L. P. Keszthelyi, pers. commun., 2006). High spatial

resolution observations at short enough wavelengths will be able to test for such temperatures during future eruptions. As techniques and telescope apertures increase (with corresponding increases in resolution) it will be possible to address additional questions.

In conclusion, observation of Io's volcanoes using data obtained by the *Galileo* spacecraft indicate that many, if not most, active volcanoes show evidence of producing both explosive and effusive deposits, and many volcanoes produce eruptions of more than one eruption style. For example, the Pele Volcano typically produces both intra-Patera and explosion-dominated events, whereas the Tvashtar Volcano was observed by *Galileo* to produce apparently all three types of eruption styles. Clearly, there is a complex and varying interaction between silicate magma with various volatile materials, including sulfur, SO<sub>2</sub>, and perhaps Cl (Schmitt and Rodriguez, 2003). Heat from silicate magmas and lavas clearly mobilizes sulfur-rich surroundings, producing both extrusive and explosive sulfurous volcanic materials. The evidence for primary effusive sulfur and sulfur dioxide flows remains equivocal. What is clear from *Galileo* observations is that most resurfacing by lava flows is confined within paterae involving probable lava lakes. In addition, while various styles of lava flow emplacement involving silicate and sulfurous flows appear to occur on Io, the dominant mechanism for resurfacing the moon as a whole is by emplacement of explosive plume deposits driven by magma-volatile interactions. Yet many questions remain: What are the hottest temperatures of erupting silicate lavas on Io? Are these lavas ultramafic or superheated basalts? How extensive are primary sulfur flows? Are there actually extrusive SO<sub>2</sub> flows, and how are they emplaced? How do paterae form and maintain connections with their magma sources? Is there an "asthenosphere", and does it allow for a subsurface connection between primary volcanic centers? Answers to these and other questions about Io's volcanism must be addressed by ground-based observing campaigns while we await future missions to the Jovian system.

## 7.6 REFERENCES

- Banfield, A. F. 1954. Volcanic deposits of elemental sulphur. *Can. Min. Metall. Bull.*, **47**, 769–775.
- Basaltic Volcanism Study Project. 1981. *Basaltic Volcanism on the Terrestrial Planets*. Pergamon Press, New York, 1286pp.
- Blaney, D. L., Johnson, T. V., Matson, D. L., and Veeder, G. J. 1995. Volcanic eruptions on Io: Heat flow, resurfacing, and lava composition. *Icarus*, **113**, 220–225.
- Blaney, D. L., Veeder, G. J., Matson, D. L., Johnson, T. K., Goguen, J. D., and Spencer, J. R. 1997. Io's thermal anomalies: Clues to their origins from comparison of ground-based observations between 1 and 20  $\mu\text{m}$ . *Geophys. Res. Lett.*, **24**, 2459–2462.
- Bonaccorso, A., Calvari, S., Coltelli, M., Del Negro, C., and Falsaperla, S. 2004. *Mt. Etna: Volcano Laboratory* (Am. Geophys. Un. Monograph, 143). American Geophysical Union, Washington, D.C., 369pp.
- Carlson, R. W., Weissman, P. R., Smythe, W. D., and Mahoney, J. C. 1992. Near-infrared mapping spectrometer experiment on Galileo. *Space Sci. Rev.*, **60**, 457–502.

- Carlson, R. W., Smythe, W. D., Lopes-Gautier, R. M. C., Davies, A. G., Kamp, L. W., Mosher, J. A., Soderblom, L. A., Leader, F. E., Mehlman, R., Clark, R. N., *et al.* 1997. The distribution of sulfur dioxide and other infrared absorbers on the surface of Io. *Geophys. Res. Lett.*, **24**, 2479–2482.
- Carr, M. H. 1986. Silicate volcanism on Io. *Journal Geophys. Res.*, **91**, 3521–3532.
- Cas, R. A. F. and Beresford, S. W. 2001. Field characteristics and erosional processes associated with komatiitic lavas: Implications for flow behavior. *Can. Mineral.*, **39**, 505–524.
- Christensen, P. R., and 11 coauthors. 2005. Evidence for magmatic evolution and diversity on Mars from infrared observations. *Nature*, **436**, doi:10.1038/nature03639.
- Clow, G. D. and Carr, M. H. 1980. Stability of sulfur slopes on Io. *Icarus*, **44**, 268–279.
- Davies, A. G. 1996. Io's volcanism: Thermo-physical models of silicate lava compared with observations of thermal emission. *Icarus*, **124**, 45–61.
- Davies, A. G. 2003. Temperature, age and crust thickness distributions of Loki Patera on Io from Galileo NIMS data: Implications for resurfacing mechanism. *Geophys. Res. Lett.*, **30**, doi:10.1029/2003GL018371.
- Davies, A. G., Keszthelyi, L. P., Williams, D. A., Phillips, C. B., McEwen, A. S., Lopes, R. M. C., Smythe, W. D., Kamp, L. W., Soderblom, L. A., and Carlson, R. W. 2001. Thermal signature, eruption style and eruption evolution at Pele and Pillan on Io. *Journal Geophys. Res.*, **106**, 33079–33104.
- de Pater, I., Marchis, F., Macintosh, B. A., Roe, H. G., Le Mignant, D., Graham, J. R., and Davies, A. G. 2004. Keck AO observations of Io in and out of eclipse. *Icarus*, **169**, 250–263.
- De Wit, M. J. and Ashwal, L. D. 1997. *Greenstone Belts*. Oxford University Press, New York, 809pp.
- Descamps, P., Arlot, J. E., Thuillot, W., Colas, F., Vu, D. T., Bouchet, P., and Hainaut, O. 1992. Observations of the volcanoes of Io, Loki and Pele, made in 1991 at the ESO during an occultation by Europa. *Icarus*, **100**, 235–244.
- Douté, S., Schmitt, B., Lopes-Gautier, R., Carlson, R., Soderblom, L., Shirley, J., and the Galileo NIMS Team. 2001. Mapping SO<sub>2</sub> frost on Io by the modeling of NIMS hyper-spectral images. *Icarus*, **149**, 107–132.
- Douté, S., Lopes, R., Kamp, L. W., Carlson, R., Schmitt, B., and the Galileo NIMS Team. 2002. Dynamics and evolution of SO<sub>2</sub> gas condensation around Prometheus-like volcanic plumes on Io as seen by the Near-Infrared Mapping Spectrometer. *Icarus*, **158**, 460–482.
- Douté, S., Lopes, R., Kamp, L. W., Carlson, R., Schmitt, B., and the Galileo NIMS Team. 2004. Geology and activity around volcanoes on Io from the analysis of NIMS spectral images. *Icarus*, **169**, 175–196.
- Fanale, F. P., Brown, R. H., Cruikshank, D. P., and Clark, R. N. 1979. Significance of absorption features in Io's IR reflectance spectrum. *Nature*, **280**, 761–763.
- Geissler, P. E., McEwen, A. S., Keszthelyi, L., Lopes-Gautier, R., Granahan, J., and Simonelli, D. P. 1999. Global color variations on Io. *Icarus*, **140**, 265–282.
- Goguen, J. D. and Sinton, W. M. 1985. Characterization of Io's volcanic activity by infrared polarimetry. *Science*, **230**, 65–69.
- Goguen, J. D., Lubenow, A., and Storrs, A. 1998. HST NICMOS images of Io in Jupiter's shadow. *Bull. Am. Astro. Soc.*, **30**, 1120.
- Goguen, J. D., Matson, D. L., Sinton, W. M., Howell, R. R., and Dyck, H. M. 1988. Io hot spots: Infrared photometry of satellite occultations. *Icarus*, **76**, 465–484.
- Greeley, R., Theilig, E., and Christensen, P. 1984. The Mauna Loa sulfur flow as an analog to secondary sulfur flows (?) on Io. *Icarus*, **60**, 189–199.

- Gregg, T. K. P. and Lopes, R. M. 2004. Lava lakes on Io: New perspectives from modeling. *Lunar & Planetary Science Conference, XXXV*, Abstract #1558.
- Hanel, R., Conrath, B., Flaser, M., Kunde, V., Lowman, P., Maguire, W., Pearl, J., Pirraglia, J., Samuelson, R., Gautier, D., Gierasch, P. *et al.* 1979. Infrared observations of the Jovian system from Voyager 1. *Science*, **204**, 972–976.
- Hansen, O. L. 1973. Ten-micron eclipse observations of Io, Europa, and Ganymede. *Icarus*, **18**, 237–246.
- Hapke, B. 1989. The surface of Io: A new model. *Icarus*, **79**, 56–74.
- Harris, A. J. L., Sherman, S. B., and Wright, R. 2000. Discovery of self-combusting volcanic sulfur flows. *Geology*, **28**, 415–418.
- Heliker, C., Swanson, D. A., and Takahashi, T. J. 2003. *The Pu'u' O'o'-Kupaianaha Eruption of Kilauea Volcano, Hawai'i: The First 20 Years* (USGS Prof. Pap., **1676**). U.S. Geological Survey, Reston, Virginia, 206pp.
- Hess, H. H. and Poldervaart, A. 1967. *Basalts: The Poldervaart Treatise on Rocks of Basaltic Composition*. Interscience Publishers, New York.
- Hill, R. E. T., Barnes, S. J., Gole, M. J., and Dowling, S. E. 1990. *Physical Volcanology of Komatiites* (Geol. Soc. Austral. (W.A. Div.) Excursion Guide Book 1). Geological Society of Australia (Western Australia Division), Perth, 100pp.
- Hill, R. E. T., Barnes, S. J., and Dowling, S. E. 2001. *Komatiites of the Norseman-Wiluna Greenstone Belt, Western Australia: A Field Guide* (Geol. Surv. West. Austral. Rec., **2001/10**). Geological Survey of Western Australia, Perth, 71pp.
- Hon, K., Kauahikaua, J., Delinger, R., and Mackay, K. 1994. Emplacement and inflation of pahoehoe sheet flows: Observations and measurements of active lava flows on Kilauea Volcano, Hawaii. *Geol. Soc. Am. Bull.*, **106**, 351–370.
- Howell, R. R. 1997. Thermal Emission from Lava Flows on Io. *Icarus*, **127**, 394–407.
- Howell, R. R. and McGinn, M. T. 1985. Infrared speckle observations of Io: An eruption in the Loki region. *Science*, **230**, 63–65.
- Howell, R. R., Spencer, J. R., Goguen, J. D., Marchis, F., Prangé, R., Fusco, T., Blaney, D. L., Veeder, G. J., Rathbun, J. A., Orton, G. S., Grocholski, A. J. *et al.* 2001. Ground-based observations of volcanism on Io in 1999 and early 2000. *J. Geophys. Res.*, **106**, 33129–33140.
- Howell, R. R. and Lopes, R. M. 2004. Characterization of activity at Loki from Galileo and ground-based observations. *Lunar & Planetary Science Conference, XXXV*, Abstract #2071.
- Huppert, H. E. and Sparks, R. S. J. 1985. Komatiites I: Eruption and flow. *J. Petrol.*, **26**, 694–725.
- Jaeger, W. L., Turtle, E. P., Keszthelyi, L. P., Radebaugh, J., and McEwen, A. S. 2003. Orogenic tectonism on Io. *J. Geophys. Res.*, **108**, doi:10.1029/2002JE001946.
- Johnson, R. E. 1997. Polar caps on Ganymede and Io revisited. *Icarus*, **128**, 469–471.
- Johnson, T. V., Morrison, D., Matson, D. L., Veeder, G. J., Brown, R. H., and Nelson, R. M. 1984. Volcanic hotspots on Io: Stability and longitudinal distribution. *Science*, **226**, 134–137.
- Johnson, T. V., Veeder, G. J., Matson, D. L., Brown, R. H., and Nelson, R. M. 1988. Io: Evidence for silicate volcanism in 1986. *Science*, **242**, 1280–1283.
- Kargel, J. S., Delmelle, P., and Nash, D. B. 1999. Volcanogenic sulfur on Earth and Io: Composition and spectroscopy. *Icarus*, **142**, 249–280.
- Kargel, J. S., and 23 coauthors. 2003. Extreme volcanism on Io: Latest insights at the end of Galileo era. *Eos*, **84**, 313, 318.

- Keszthelyi, L., McEwen, A. S., Phillips, C. B., Milazzo, M., Geissler, P., Turtle, E. P., Radebaugh, J., Williams, D. A., Simonelli, D., Breneman, H. *et al.* 2001. Imaging of volcanic activity on Jupiter's moon Io by Galileo during GEM and GMM. *J. Geophys. Res.*, **106**, 33025–33052.
- Kieffer, S. W., Lopes-Gautier, R., McEwen, A., Smythe, W., Keszthelyi, L., and Carlson, R. 2000. Prometheus: Io's wandering plume. *Science*, **288**, 1204–1208.
- Klaasen, K. P., Clary, M. C., and Janesick, J. R. 1984. Charge-coupled device television camera for NASA's Galileo Mission to Jupiter. *Opt. Eng.*, **23**, 334–342.
- Kupo, I., Mekler, Y., and Eviatar, A. 1976. Detection of ionized sulfur in the Jovian magnetosphere. *Astrophys. Journal Lett.*, **205**, L51–L53.
- Lopes-Gautier, R., McEwen, A. S., Smythe, W. B., Geissler, P. E., Kamp, L., Davies, A. G., Spencer, J. R., Keszthelyi, L., Carlson, R., Leader, F. E., *et al.* 1999. Active Volcanism on Io: Global distribution and variations in activity. *Icarus*, **140**, 243–264.
- Lopes-Gautier, R., Douté, S., Smythe, W. D., Kamp, L. W., Carlson, R. W., Davies, A. G., Leader, F. E., McEwen, A. S., Geissler, P. E., Kieffer, S. W., *et al.* 2000. A close-up look at Io in the infrared: Results from Galileo's Near-Infrared Mapping Spectrometer. *Science*, **288**, 1201–1204.
- Lopes, R. M. C., Kamp, L. W., Douté, S., Smythe, W. D., Carlson, R. W., McEwen, A. S., Geissler, P. E., Kieffer, S. W., Leader, F. E., Davies, A. G., *et al.* 2001. Io in the near-infrared: NIMS results from the Galileo fly-bys in 1999 and 2000. *J. Geophys. Res.*, **106**, 33053–33078.
- Lopes, R. M. C., Kamp, L. W., Davies, A. G., Smythe, W. D., Carlson, R. W., Douté, S., McEwen, A., Turtle, E. P., Leader, F., Mehlman, R., *et al.* 2002. Galileo's last fly-bys of Io: NIMS observations of Loki, Tupan, and Emakong calderas. *Lunar & Planetary Science Conference*, **XXXIII**, Abstract #1739.
- Lopes, R. M. C., Kamp, L. W., Smythe, W. D., Mouginiis-Mark, P., Kargel, J., Radebaugh, J., Turtle, E. P., Perry, J., Williams, D. A., Carlson, R. W., *et al.* 2004. Lava lakes on Io: Observations of Io's volcanic activity from Galileo NIMS during the 2001 fly-bys. *Icarus*, **169**, 140–174.
- MacDonald, G. A. 1967. Forms and structures of extrusive basaltic rocks. In: Hess, H. H. and Poldervaart, A. (eds), *Basalts: The Poldervaart Treatise on Rocks of Basaltic Composition*. Interscience Publishers, New York, pp. 1–58.
- McBirney, A. R. 1993. *Igneous Petrology*. Jones & Bartlett Publishers, London, 508pp.
- McEwen, A. S. and Soderblom, L. A. 1983. Two classes of volcanic plumes on Io. *Icarus*, **55**, 191–217.
- McEwen, A. S., Soderblom, L. A., Matson, D. L., and Johnson, T. V. 1985. Volcanic hot spots on Io: Correlation with low-albedo calderas. *J. Geophys. Res.*, **90**, 12345–12379.
- McEwen, A. S., Keszthelyi, L., Geissler, P., Simonelli, D. P., Carr, M. H., Johnson, T. V., Klaasen, K. P., Breneman, H. H., Jones, T. J., Kaufman, J. M., *et al.* 1998a. Active volcanism on Io as seen by Galileo SSI. *Icarus*, **135**, 181–219.
- McEwen, A. S., Keszthelyi, L., Spencer, J. R., Schubert, G., Matson, D. L., Lopes-Gautier, R., Klaasen, K. P., Johnson, T. V., Head, J. W., Geissler, P., *et al.* 1998b. High-temperature silicate volcanism on Jupiter's moon Io. *Science*, **281**, 87–90.
- McEwen, A. S., Belton, M. J. S., Breneman, H. H., Fagents, S. A., Geissler, P., Greeley, R., Head, J. W., Hoppa, G., Jaeger, W. L., Johnson, T. V. *et al.* 2000. Galileo at Io: Results from high-resolution imaging. *Science*, **288**, 1193–1198.
- McLeod, B. A., McCarthy, D. W., Jr., and Freeman, J. 1991. Global high-resolution imaging of hotspots on Io. *Astronom. Journal*, **102**, 1485–1489.

- Marchis, F., Prangé, R., and Christou, J. 2000. Adaptive optics mapping of Io's volcanism in the thermal IR (3.8  $\mu\text{m}$ ). *Icarus*, **148**, 384–396.
- Marchis, F., Prangé, R., and Fusco, T. 2001. A survey of Io's volcanism by adaptive optics observations in the 3.8- $\mu\text{m}$  thermal band (1996–1999). *J. Geophys. Res.*, **106**, 33141–33160.
- Marchis, F., de Pater, I., Davies, A. G., Roe, H. G., Fusco, T., Le Mignant, D., Descamps, P., Macintosh, B. A., and Prangé, R. 2002. High-resolution Keck adaptive optics imaging of violent volcanic activity on Io. *Icarus*, **160**, 124–131.
- Matson, D. L., Ransford, G. A., and Johnson, T. V. 1981. Heat flow from Io J1. *J. Geophys. Res.*, **86**, 1664–1672.
- Medina, F., Echevarria, J., Ledezma, E., and Martinez, F. 1989. Infrared observations of Io during the mutual events of 1985: Evidence of volcanic activity? *Astronomy and Astrophysics*, **220**, 313–317.
- Milazzo, M. P., Keszthelyi, L. P., and McEwen, A. S. 2001. Observations and initial modeling of lava–SO<sub>2</sub> interactions at Prometheus, Io. *J. Geophys. Res.*, **106**, 33121–33128.
- Milazzo, M. P., Keszthelyi, L. P., Radebaugh, J., Davies, A. G., Turtle, E. P., Geissler, P., Klaasen, K. P., Rathbun, J. A., and McEwen, A. S. 2005. Volcanic activity at Tvashtar Catena, Io. *Icarus*, **179**, 235–251.
- Morabito, L. A., Synnott, S. P., Kupferman, P. N., and Collins, S. A. 1979. Discovery of currently active extraterrestrial volcanism. *Science*, **204**, 972.
- Morrison, D. and Cruikshank, D. P. 1973. Thermal properties of the Galilean satellites. *Icarus*, **18**, 224–236.
- Morrison, D. and Telesco, C. M. 1980. Io: Observational constraints on internal energy and thermophysics of the surface. *Icarus*, **44**, 226–233.
- Morrison, D., Pieri, D., Johnson, T. V., and Veverka, J. 1979. Photometric evidence on long-term stability of albedo and colour markings on Io. *Nature*, **280**, 753–755.
- Naranjo, J. A. 1985. Sulphur flows at Lastarria volcano in the North Chilean Andes. *Nature*, **313**, 778–780.
- Nash, D. B. 1987. Sulfur in vacuum: Sublimation effects on frozen melts, and applications to Io's surface and torus. *Icarus*, **72**, 1–34.
- Nash, D. B. and Nelson, R. M. 1979. Spectral evidence for sublimates and adsorbates on Io. *Nature*, **280**, 763–766.
- Oppenheimer, C. 1992. Sulphur eruptions at Volcán Poás, Costa Rica. *J. Volcanol. Geotherm. Res.*, **49**, 1–21.
- O'Reilly, T. C. and Davies, G. F. 1981. Magma transport of heat on Io: A mechanism allowing a thick lithosphere. *Geophys. Res. Lett.*, **8**, 313–316.
- Peale, S. J., Cassen, P., and Reynolds, R. T. 1979. Melting of Io by tidal dissipation. *Science*, **203**, 892–894.
- Pearl, J. C. and Sinton, W. M. 1982. Hot spots of Io. In: D. Morrison and M. S. Matthews (eds), *Satellites of Jupiter*. University of Arizona Press, Tucson, AZ, pp. 724–755.
- Pearl, J., Hanel, R., Kunde, V., Maguire, W., Fox, K., Gupta, S., Ponnampuruma, C., and Raulin, F. 1979. Identification of gaseous SO<sub>2</sub> and new upper limits for other gases on Io. *Nature*, **280**, 755–758.
- Pieri, D., Baloga, S. M., Nelson, R. M., and Sagan, C. 1984. Sulfur flows of Ra Patera, Io. *Icarus*, **60**, 685–700.
- Radebaugh, J., Keszthelyi, L. P., McEwen, A. S., Turtle, E. P., Jaeger, W., and Milazzo, M. 2001. Paterae on Io: A new type of volcanic caldera? *J. Geophys. Res.*, **106**, 33005–33020.

- Radebaugh, J., McEwen, A. S., Milazzo, M. P., Keszthelyi, L. P., Davies, A. G., Turtle, E. P., and Dawson, D. D. 2004. Observations and temperatures of Io's Pele Patera from Cassini and Galileo spacecraft images. *Icarus*, **169**, 65–79.
- Rathbun, J. A., Spencer, J. R., Davies, A. G., Howell, R. R., and Wilson, L. 2002. Loki, Io: A periodic volcano. *Geophys. Res. Lett.*, **29**(10), 10.1029/2002GL014747.
- Rathbun, J. A., Johnson, S. T., and Spencer, J. R. 2003. Loki, Io: An update from ground-based data. *Lunar & Planetary Science Conference*, **XXXIV**, Abstract #1375.
- Reidel, S. P. and Hooper, P. R. 1989. *Volcanism and Tectonism in the Columbia River Flood Basalt Province* (Geol. Soc. Am. Sp. Pap., **239**). Geological Society of America, Boulder, 386pp.
- Rhodes, J. M. and Lockwood, J. P. 1995. *Mauna Loa Revealed: Structure, Composition, History, and Hazards* (Am. Geophys. Un. Monograph, **92**). American Geophysical Union, Washington, D.C., 348pp.
- Ross, M. N., Schubert, G., Spohn, T., and Gaskell, R. W. 1990. Internal structure of Io and the global distribution of its topography. *Icarus*, **85**, 309–325.
- Sagan, C. 1979. Sulphur flows on Io. *Nature*, **280**, 750–753.
- Schaber, G. G. 1982. The geology of Io. In: Morrison, D. and Matthews, M. S. (eds), *Satellites of Jupiter*. University of Arizona Press, Tucson, TX, pp. 556–597.
- Schenk, P. M., Hargitai, H., Wilson, R., McEwen, A., and Thomas, P. 2001. The mountains of Io: Global and geological perspectives from Voyager and Galileo. *J. Geophys. Res.*, **106**, 33201–33222.
- Schmitt, B. and Rodriguez, S. 2003. Possible identification of local deposits of  $\text{Cl}_2\text{SO}_2$  on Io from NIMS/Galileo spectra. *J. Geophys. Res.*, **108**(E9), 5104, doi:10.1029/2002JE001988.
- Schmincke, H.-U. 2004. *Volcanism*. Springer, Berlin, 324pp.
- Self, S., Thordarson, T., and Keszthelyi, L. 1997. Emplacement of continental flood basalt lava flows. In: J. J. Mahoney and M. F. Coffin (eds), *Large Igneous Provinces: Continental, Oceanic, and Planetary Flood Volcanism* (Am. Geophys. Un. Monograph, **100**). American Geophysical Union, Washington, D.C., pp. 381–410.
- Shaw, H. R. and Swanson, D. A. 1970. Eruption and flow rates of flood basalts. In: Gilmour, E. H. and Stradling, D. (eds), *Proceedings of the 2nd Columbia River Basalt Symposium*. East Washington State Press, Cheney, pp. 271–299.
- Sinton, W. M. 1980. Io's 5 micron variability. *Astrophys. Journal Lett.*, **235**, L49–L51.
- Sinton, W. M. 1981. The thermal emission spectrum of Io and a determination of the heat flux from its hot spots. *J. Geophys. Res.*, **86**, 3122–3128.
- Sinton, W. M., Tokunaga, A. T., Becklin, E. E., Gatley, I., Lee, T. J., and Lonsdale, C. J. 1980. Io: Ground-based observations of hot spots. *Science*, **210**, 1015–1017.
- Sinton, W. M., Lindwall, D., Cheigh, F., and Tittlemore, W. C. 1983. Io: The near-infrared monitoring program, 1979–1981. *Icarus*, **54**, 133–157.
- Skinner, B. J. 1970. A sulfur lava flow on Mauna Loa. *Pac. Sci.*, **24**, 144–145.
- Smellie, J. L. and Chapman, M. G. 2002. *Volcano-Ice Interaction on Earth and Mars* (Geol. Soc. Sp. Pub., **202**). The Geological Society, London, 431pp.
- Smith, B. A., Soderblom, L. A., Johnson, T. V., Ingersoll, A. P., Collins, S. A., Shoemaker, E. M., Hunt, G. E., Masursky, H., Carr, M. H., Davies, M. E. *et al.* 1979. The Jupiter system through the eyes of Voyager 1. *Science*, **204**, 951–957.
- Smythe, W. D., Nelson, R. M., and Nash, D. B. 1979. Spectral evidence for  $\text{SO}_2$  frost or adsorbate on Io's surface. *Nature*, **280**, 766.
- Smythe, W. D., Lopes-Gautier, R., Ocampo, A., Hui, J., Segura, M., Soderblom, L. A., Matson, D. L., Kieffer, H. H., McCord, T. B., Fanale, F. P., *et al.* 1995. Galilean

- satellite observation plans for the near-infrared mapping spectrometer experiment on the Galileo spacecraft. *J. Geophys. Res.*, **100**, 18957–18972.
- Smythe, W. D., Lopes-Gautier, R., Douté, S., Kieffer, S. W., Carlson, R. W., Kamp, L., and Leader, F. E. 2000. Evidence for massive sulfur dioxide deposit on Io. *Bull. Am. Astron. Soc.*, **32**(3), 1047.
- Spencer, J. R., Shure, M. A., Ressler, M. E., Sinton, W. M., and Goguen, J. D. 1990. Discovery of hotspots on Io using disk-resolved infrared imaging. *Nature*, **348**, 618–621.
- Spencer, J. R., Clark, B. E., Toomey, D., Woodney, L. M., and Sinton, W. M. 1994. Io hot spots in 1991: Results from Europa occultation photometry and infrared imaging. *Icarus*, **107**, 195–208.
- Spencer, J. R., McEwen, A. S., McGrath, M. A., Sartoretti, P., Nash, D. B., Noll, K. S., and Gilmore, D. 1997. Volcanic resurfacing of Io: Post-repair HST imaging. *Icarus*, **127**, 221–237.
- Spencer, J. R., Jessup, K. L., McGrath, M. A., Ballester, G. E., and Yelle, R. 2000a. Discovery of gaseous S<sub>2</sub> in Io's Pele plume. *Science*, **288**, 1208–1210.
- Spencer, J. R., Rathbun, J. A., Travis, L. D., Tamppari, L. K., Barnard, L., Martin, T. Z., and McEwen, A. S. 2000b. Io's thermal emission from the Galileo Photopolarimeter–Radiometer. *Science*, **288**, 1198–1201.
- Stansberry, J. A., Spencer, J. R., Howell, R. R., Dumas, C., and Vakil, D. 1997. Violent silicate volcanism on Io in 1996. *Geophys. Res. Lett.*, **24**, 2455–2458.
- Stuedel, R., Holdt, G., and Young, A. T. 1986. On the colors of Jupiter's satellite Io: Irradiation of solid sulfur at 77 K. *J. Geophys. Res.*, **91**, 4971–4977.
- Tackley, P. J., Schubert, G., Glatzmaier, G. A., Schenk, P., Ratcliff, J. T., and Matas, J.-P. 2001. Three dimensional simulations of mantle convection in Io. *Icarus*, **149**, 79–91.
- Theilig, E. 1982. A primer on sulfur for the planetary geologist (NASA Contractor Report 3594). NASA, Reston, VA, 34pp.
- Thordarson, T. and Self, S. 1993. The Laki (Skaftár Fires) and Grímsvötn eruptions in 1783–1785. *Bull. Volcanol.*, **55**, 233–263.
- Thordarson, T. and Self, S. 1998. The Roza Member, Columbia River Basalt Group: A gigantic pahoehoe lava flow field formed by endogeneous processes? *J. Geophys. Res.*, **103**, 27411–27445.
- Turtle, E. P., Keszthelyi, L. P., McEwen, A. S., Radebaugh, J., Milazzo, M., Simonelli, D. P., Geissler, P., Williams, D. A., Perry, J., Jaeger, W. L. *et al.* 2004. The final Galileo SSI observations of Io: Orbits G28-I33. *Icarus*, **169**, 3–28.
- Veeder, G. J., Matson, D. L., Johnson, T. V., Blaney, D. L., and Goguen, J. D. 1994. Io's heat flow from infrared radiometry: 1983–1993. *J. Geophys. Res.*, **99**, 17095–17162.
- Watanabe, T. 1940. Eruptions of molten sulphur from the Siretoko-Isan Volcano, Hokkaid, Japan. *Jpn. J. Geol. Geog.*, **17**, 289–310.
- Wentworth, C. K. and Macdonald, G. A. 1953. Structures and forms of basaltic rocks in Hawaii. *U.S. Geol. Surv. Bull.*, **994**, 1–98.
- Williams, D. A., Wilson, A. H., and Greeley, R. 2000a. A komatiite analog to potential ultramafic materials on Io. *J. Geophys. Res.*, **105**, 1671–1684.
- Williams, D. A., Fagents, S. A., and Greeley, R. 2000b. A reassessment of the emplacement and erosional potential of turbulent, low-viscosity lavas on the Moon. *J. Geophys. Res.*, **105**, 20189–20205.
- Williams, D. A., Davies, A. G., Keszthelyi, L. P., and Greeley, R. 2001a. The summer 1997 eruption at Pillan Patera on Io: Implications for ultrabasic lava flow emplacement. *J. Geophys. Res.*, **106**, 33105–33119.

- Williams, D. A., Greeley, R., Lopes-Gautier, R. M. C., and Douté, S. 2001b. Evaluation of sulfur flow emplacement on Io from Galileo data and numerical modeling. *J. Geophys. Res.*, **106**, 33161–33174.
- Williams, D. A., Radebaugh, J., Keszthelyi, L. P., McEwen, A. S., Lopes, R. M. C., Douté, S. and Greeley, R. 2002. Geologic mapping of the Chaac-Camaxtli region of Io from Galileo imaging data. *J. Geophys. Res.*, **107**, 5068, doi:10.1029/2001JE001821.
- Williams, D. A., Schenk, P. M., Moore, J. M., Keszthelyi, L. P., Turtle, E. P., Jaeger, W. L., Radebaugh, J., Milazzo, M. P., Lopes, R. M. C., and Greeley, R. 2004. Mapping of the Culann-Tohil region of Io from Galileo imaging data. *Icarus*, **169**, 80–97.
- Witteborn, F. E., Bregman, J. D., and Pollack, J. B. 1979. Io: An intense brightening near 5 micrometers. *Science*, **203**, 643–646.
- Yoder, C. F. 1979. How tidal heating in Io drives the Galilean orbital resonance locks. *Nature*, **279**, 767–770.
- Young, A. T. 1984. No sulfur flows on Io. *Icarus*, **58**, 197–226.
- Zimbelman, J. R. and Gregg, T. K. P. 2000. *Environmental Effects on Volcanic Eruptions: From Deep Oceans to Deep Space*. Kluwer Academic/Plenum Publishers, New York, 260pp.

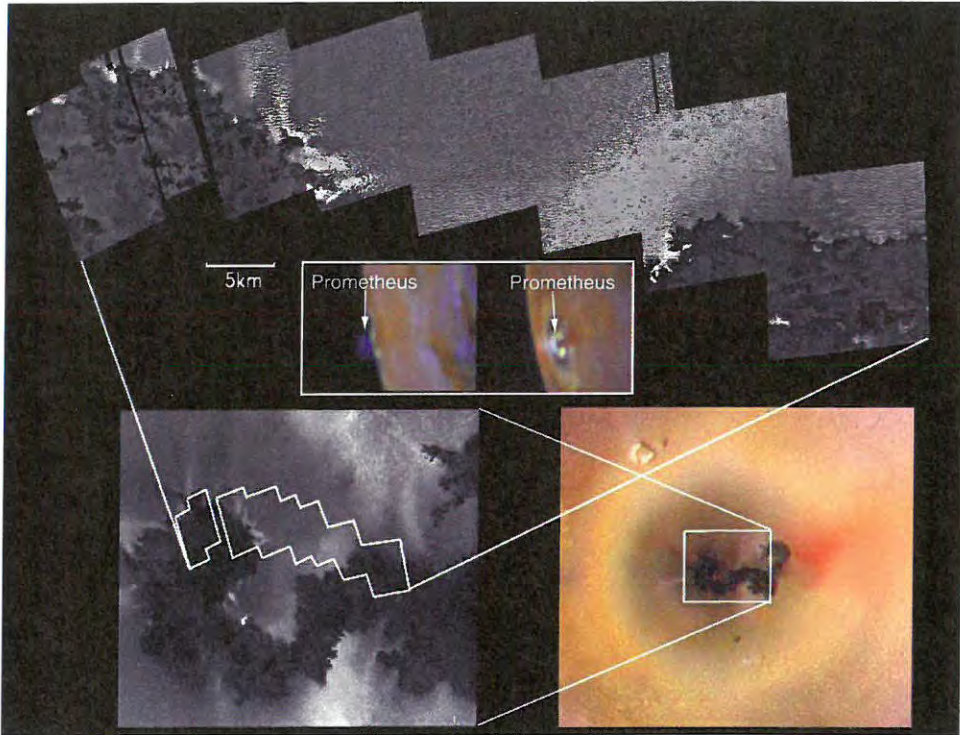


**Figure 7.2.** A montage of *Galileo* SSI images of the Prometheus volcano at several different resolutions, which identify various aspects of the flow-dominated eruption style. These eruptions produce compound silicate flow fields that are slowly emplaced over months to years, with measured temperatures consistent with terrestrial basaltic volcanism (Keszthelyi *et al.*, 2001). Note the small dark patches in the flow field indicative of recent breakouts. Heat from advancing flows vaporizes  $\text{SO}_2$  snow producing jet-like flow front plumes (Kieffer *et al.*, 2000; Milazzo *et al.*, 2001). The central inset shows examples of the Prometheus plume.

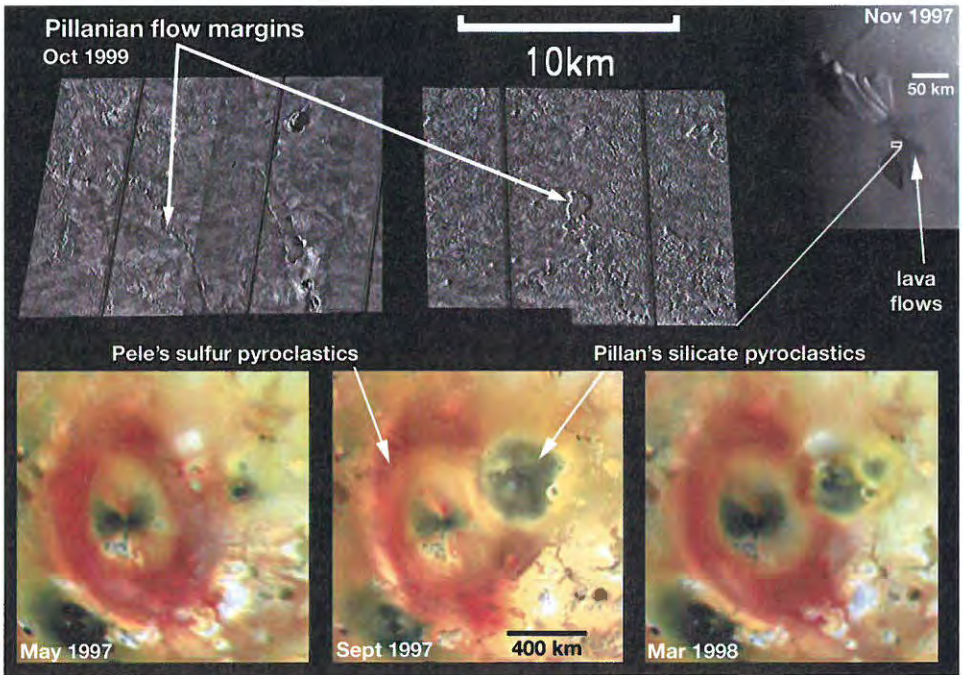


**Figure 7.4.** A montage of *Galileo* SSI images of the Pillan volcano at several different resolutions, which identify various aspects of an explosion-dominated (formerly Pillanian) eruption style. (*top*) The Pillan lava flow field, which emanated from fissures that fracture a mountain north of the caldera. (*bottom*) Changes to Pillan's surroundings (including Pele's red ring) due to activity at these volcanoes. These eruptions produce extensive flow fields that are rapidly emplaced over days to weeks, with measured temperatures consistent with terrestrial mafic to ultramafic volcanism (Keszthelyi *et al.*, 2001).

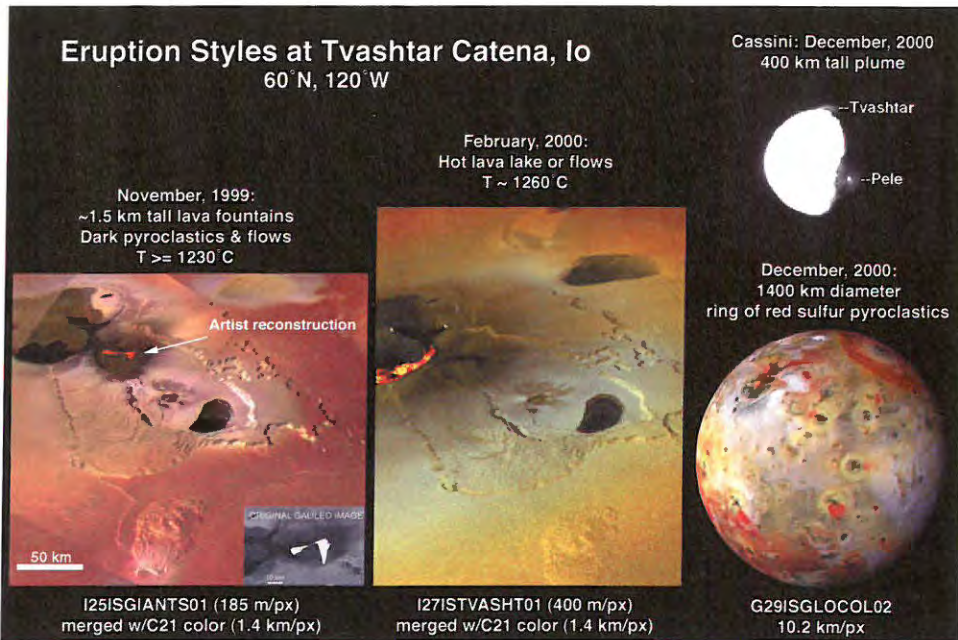


**Figure 7.5.** A montage of *Galileo* SSI and *Cassini* imaging science subsystem (ISS) images showing a range of eruption styles at Tvashtar. In November 1999 Tvashtar had a possibly flow-dominated eruption, producing a lava fountain and flow field. In February 2000 an intra-patera eruption could have occurred, producing fresh material in a lava lake (or possibly just a confined lava flow). In December 2000, the *Cassini* spacecraft recorded an explosion-dominated eruption, from which *Galileo* imaged a large red ring deposit of sulfur. It remains unclear whether any new flows were emplaced (rapidly or otherwise) after the December 2000 event.

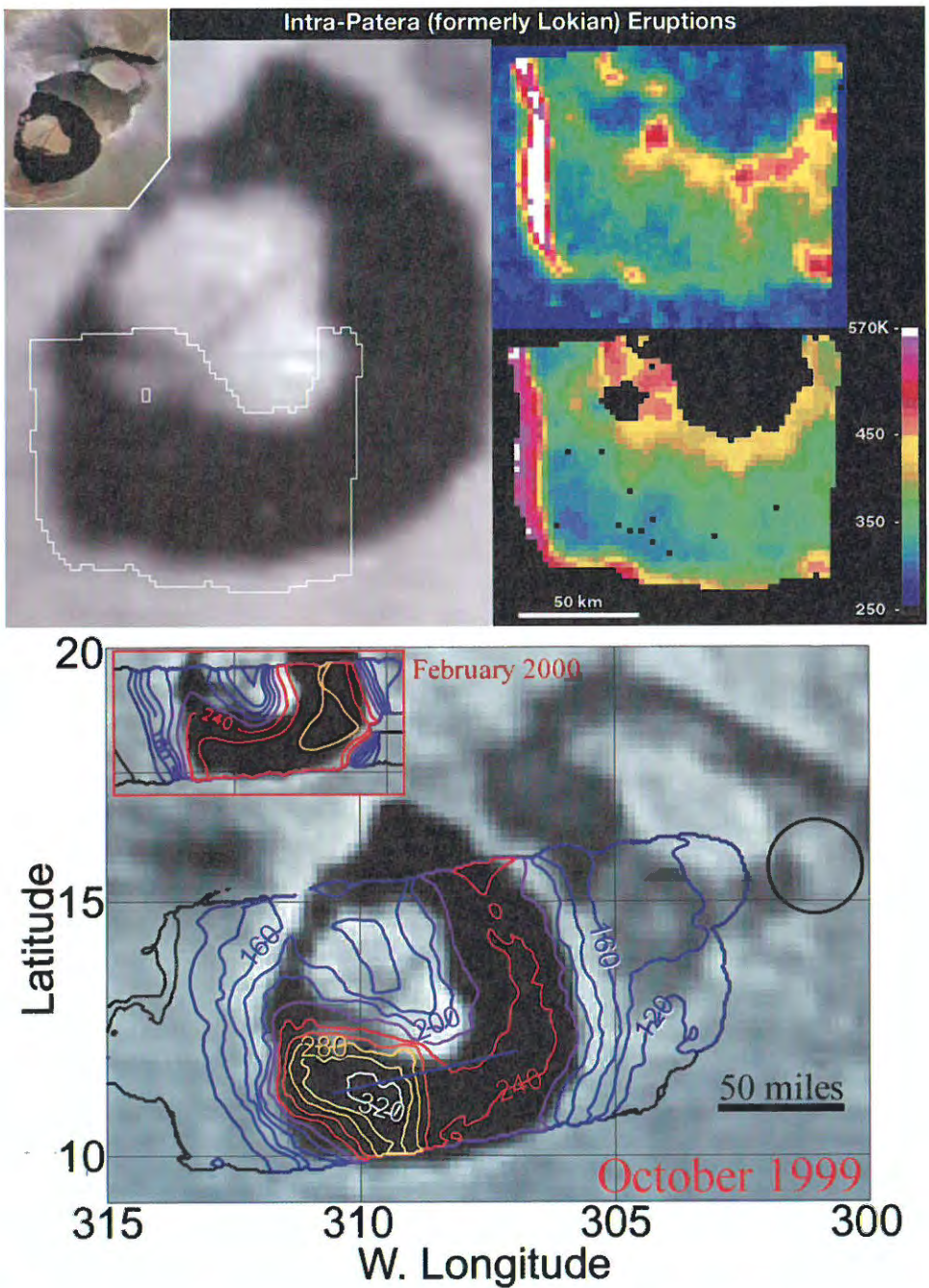


**Figure 7.6.** A montage of *Voyager* and *Galileo* SSI, NIMS, and PPR images of Loki volcano at several different resolutions and times, which identify various aspects of an intra-patera (formerly Lokian) eruption style. These eruptions produce lava lakes that are overturned over months to years, with measured temperatures typically consistent with terrestrial basaltic volcanism (Lopes *et al.*, 2004). The color panel at upper right is a NIMS map at  $2.5\ \mu\text{m}$  showing a hot edge (white:  $T \sim 840\ \text{K}$ ) at the western wall, whereas the image at lower right is a NIMS temperature map showing warmer and cooler parts of the patera floor. The bottom image shows PPR data over an image of Loki, showing the migration of the hottest part of the patera floor from west to east (from Spencer *et al.*, 2000b).

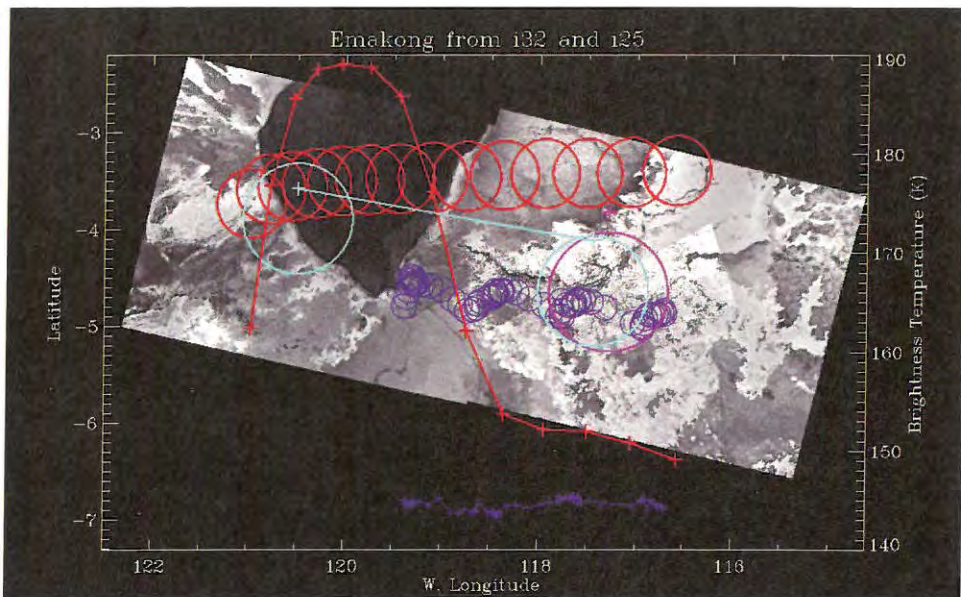


**Figure 7.7.** *Galileo* PPR data superposed upon SSI images of Emakong Patera. The PPR data demonstrate the very cold surface of the floor of Emakong Patera and its surrounding bright flows. NIMS data also showed that  $\text{SO}_2$  frost is stable on parts of the patera floor, which suggests that Emakong may represent a cooled, inactive sulfur volcano (or, alternatively, a very cooled silicate volcano with silicate flows heavily mantled by sulfurous deposits: Williams *et al.*, 2001b).

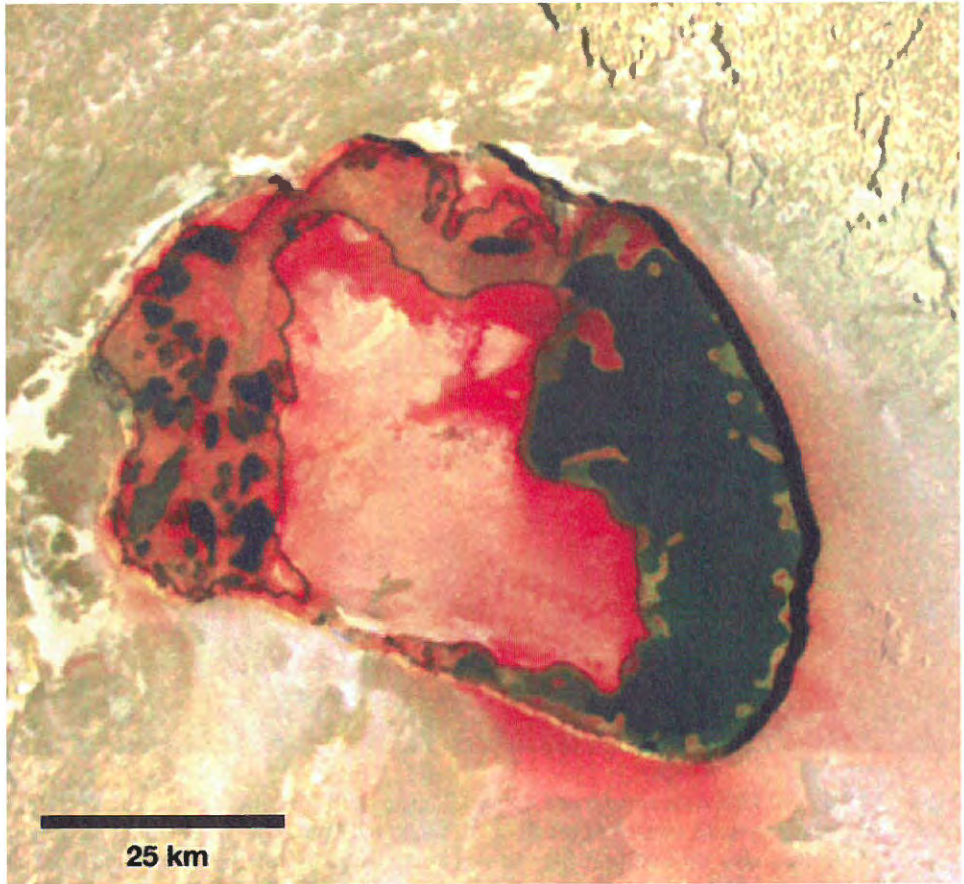


**Figure 7.8.** *Galileo* SSI image of Tupa Patera obtained in October 2001, another example of an intra-patera eruption style. Heat from the lava lake appears to melt bright sulfur deposits along the margins of the lake, which accumulate as bright “puddles” on the dark surface of the lake. Diffuse red deposits, presumably short-chain sulfur crystallized from  $S_2$  gas, cover the margins of the patera and large parts of the central island. This is the highest resolution color image of Io obtained during the *Galileo* mission (132 m per pixel).

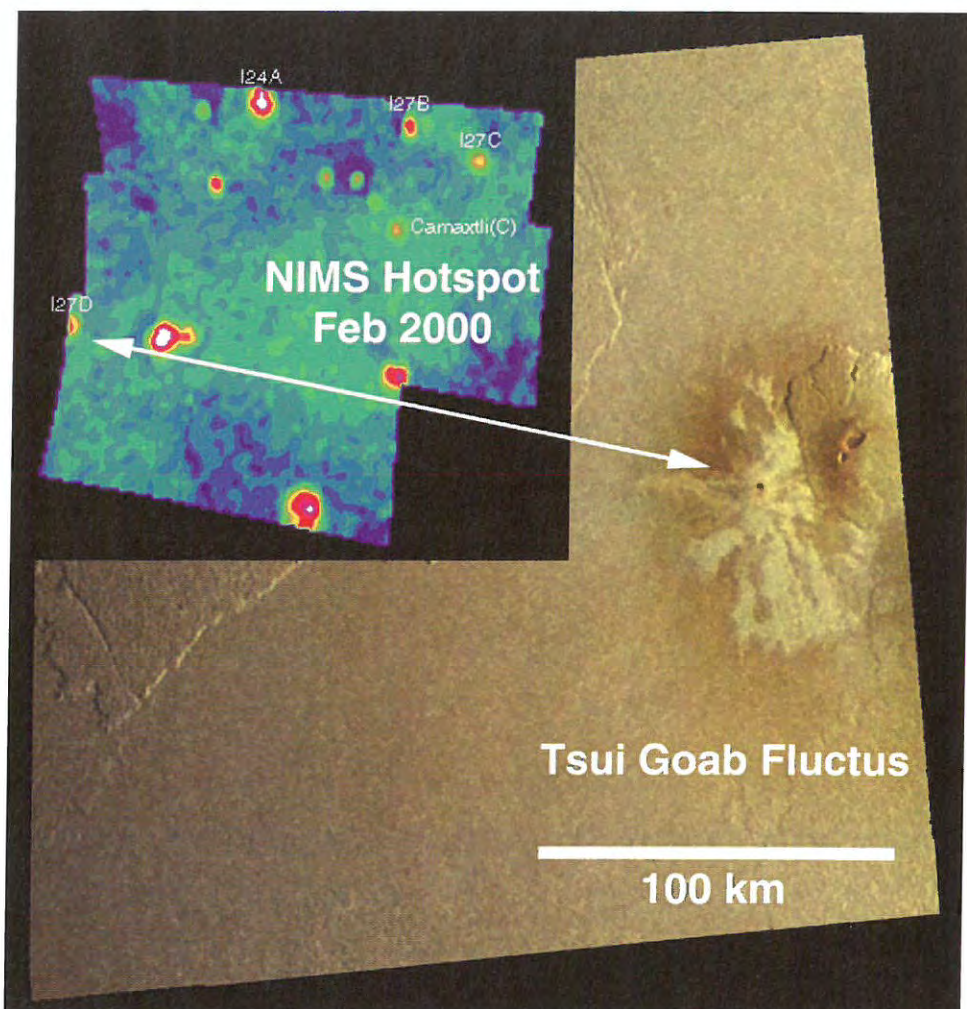


**Figure 7.9.** Low-resolution NIMS hot spot image (*inset*), with white arrows showing the correlation of the I27D hot spot of Lopes *et al.* (2001) with the bright flow field of Tsui Goab Fluctus in the Culann-Tohil region as imaged by the SSI during October 2001. This is the only location of potentially active, primary sulfur effusive volcanism detected during the *Galileo* mission.

## Possible Sites of Effusive Sulfur Dioxide Volcanism

Balder Patera



Tohil Patera

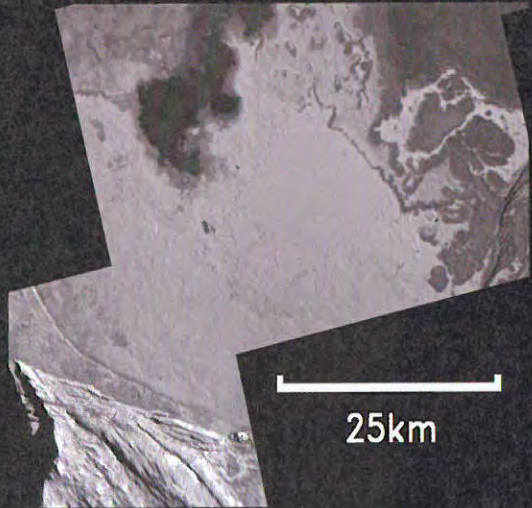


**Figure 7.10.** Galileo SSI images showing possible sites of effusive  $\text{SO}_2$  volcanism on Io. (left) Balder Patera in the Chaac-Camaxtli region (Williams *et al.*, 2002), site of a proposed glacial-like flow (Smythe *et al.*, 2000). (right) Tohil Patera in the Culann-Tohil region (Williams *et al.*, 2004), the south-west section of which has an enhanced  $\text{SO}_2$  signature and flow-like margins in its interior.